Downloaded from gsabulletin.gsapubs.org on January 7, 2013

Latest Pleistocene and Holocene slip rate for the San Bernardino strand of the San Andreas fault, Plunge Creek, Southern California: Implications for strain partitioning within the southern San Andreas fault system for the last ~35 k.y.

Sally F. McGill[1,†], Lewis A. Owen[2,†], Ray J. Weldon II[3,†], and Katherine J. Kendrick[4,†]

[1]*Department of Geological Sciences, California State University–San Bernardino, 5500 University Parkway, San Bernardino, California 92407-2397, USA*

[2]*Department of Geology, University of Cincinnati, Cincinnati, Ohio 45221-0013, USA*

[3]*Department of Geological Science, University of Oregon, Eugene, Oregon 97403-1272, USA*

[4]*U.S. Geological Survey, 525 South Wilson Avenue, Pasadena, California 91106, USA*

ABSTRACT

An alluvial succession on the northeast side of the San Bernardino strand of the San Andreas fault includes distinctive aggradational and degradational features that can be matched with correlative features on the southwest side of the fault. Key among these are (1) a terrace riser on the northeast side of the fault that correlates with an offset channel wall on the southwest side of the fault and forms a basis for slip estimates for the period ca. 35 ka to the present, and (2) a small alluvial fan on the southwest side of the fault that has been matched with its most likely source gullies on the northeast side of the fault and forms a basis for slip estimates for the last 10.5 k.y. Slip-rate estimates for these two separate intervals are nearly identical. The rate for the older feature is most likely between 8.3 and 14.5 mm/yr, with a 95% confidence interval of 7.0–15.7 mm/yr. The rate for the younger feature is most likely between 6.8 and 16.3 mm/yr, with a 95% confidence interval of 6.3–18.5 mm/yr.

These rates are only half the previously published slip rate for the San Andreas fault 35 km to the northwest in Cajon Pass, a rate that traditionally is extrapolated southeastward along the San Bernardino section of the fault. Results from Plunge Creek suggest that about half of the 25 mm/yr rate at Cajon Pass transfers southeastward to the San Jacinto fault, as proposed by other workers on the basis of regional geologic relations. These results indicate that the discrepancy between latest Quaternary slip rates and present-day rates of strain accumulation across the San Bernardino section of the San Andreas fault from geodesy can be largely explained by slip transfer between faults, leading to spatial variation in rate along the San Andreas fault. Nonetheless, the latest Pleistocene and Holocene slip rate at Plunge Creek is still somewhat faster than rates inferred for the San Bernardino section of the San Andreas fault based on elastic block modeling of geodetic data and may be more appropriate than those rates for hazard estimation.

INTRODUCTION

Despite more than 100 yr of study, significant questions remain regarding how late Quaternary strain has been distributed among the faults of the San Andreas fault system within the overall boundary between the North American and Pacific plates. The total rate of relative motion between these plates in Southern California is 52 ± 2 mm/yr (DeMets and Dixon, 1999), but geologic, geodetic, and seismologic communities have not agreed about the way in which this strain is partitioned among the various faults of the southern San Andreas system. This is especially true during the Holocene and latest Pleistocene, the interval most germane to evaluating seismic risk and modeling future earthquake ruptures. Bedrock offsets along the San Andreas fault are an order of magnitude larger than for the (younger) San Jacinto fault (Matti and Morton, 1993; Sharp, 1967), but the relative significance of the two faults in terms of present-day activity and seismic hazard remains an unresolved question. Published slip rates for the two faults measured over different time scales suggest possible temporal variations in slip rate for one or both faults, but the significance and cause of these variations and their implications for seismic hazard remain unclear.

Quaternary Strain Rates: Geologic Evidence

Between central and Southern California, the San Andreas fault zone has significant differences in structural complexity, fault-strand development, and long-term strain partitioning. These differences are associated with an ~250-km-long segment of the San Andreas fault that is oblique to the northwestward direction of relative plate motion. This restraining segment is bounded by two bends in the fault, a northern bend colloquially referred to as the "Big Bend" (Fig. 1, inset, BB), and a southern bend in San Gorgonio Pass, which is characterized by significant structural complexity in the southern San Andreas fault zone (Fig. 1, inset, SGP). North of the Big Bend, the San Andreas fault is the dominant fault within the plate boundary, and here the fault's Carrizo section has a Holocene slip rate of ~35 mm/yr (Sieh and Jahns, 1984). Within the restraining segment of the fault, northwestward motion of the Pacific plate relative to the North American plate has resulted in a complex regional pattern of faults, including (1) multiple dextral faults of the San Andreas system, (2) the Eastern California shear zone (a domain of subparallel northwest-striking dextral faults in the Mojave Desert), (3) thrust and reverse faults within the Transverse Ranges (including the San Gabriel and San Bernardino

[†]E-mails: smcgill@csusb.edu; lewis.owen@uc.edu; ray@uoregon.edu; kendrick@gps.caltech.edu

GSA Bulletin; January/February 2013; v. 125; no. 1/2; p. 48–72; doi: 10.1130/B30647.1; 15 figures; 4 tables; Data Repository item 2012288.

For permission to copy, contact editing@geosociety.org
© 2013 Geological Society of America

Downloaded from gsabulletin.gsapubs.org on January 7, 2013

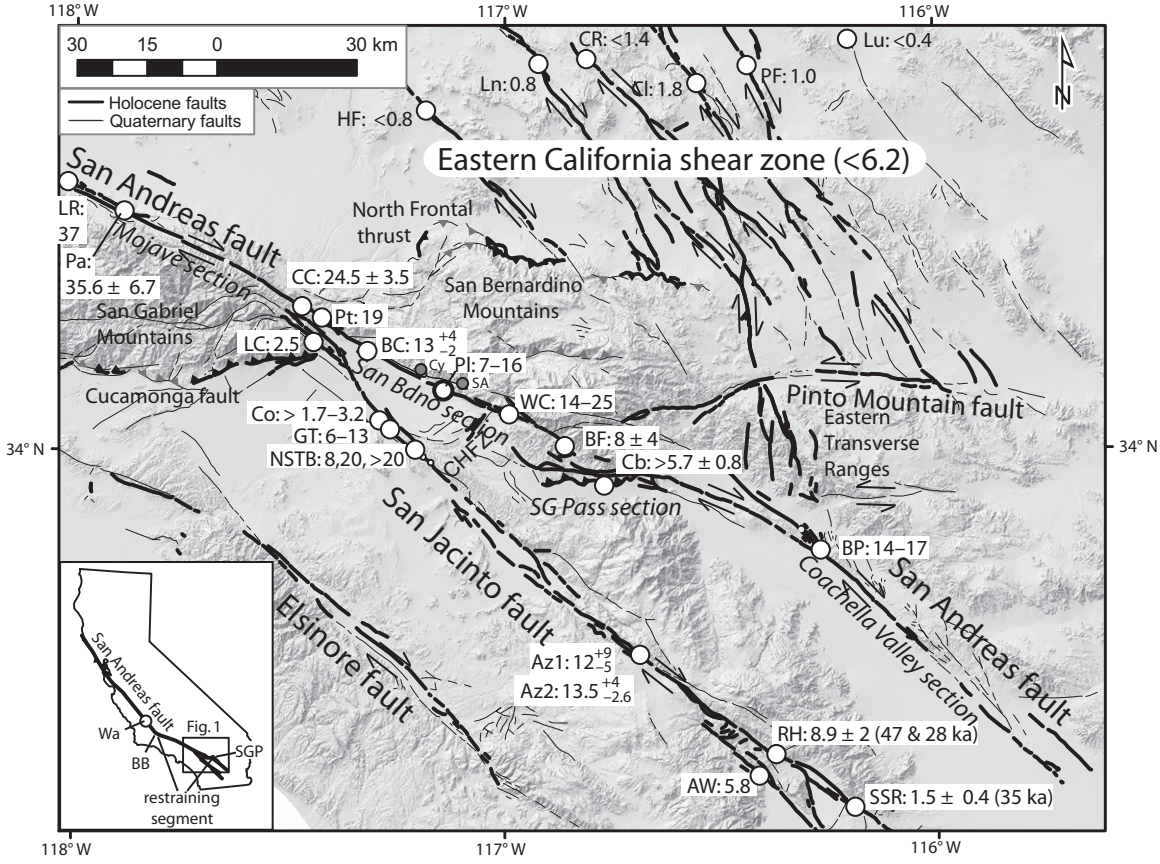

Figure 1. Major faults and fault sections discussed in text. The San Gabriel and San Bernardino Mountains are a part of the Transverse Ranges. Bold black lines show faults having Holocene activity; thinner, gray lines show faults having most recent activity during the Pleistocene (U.S. Geological Survey and California Geological Survey, 2006). White circles show locations of latest Pleistocene and Holocene slip-rate sites for the San Andreas and San Jacinto faults, with slip-rate estimates in mm/yr. Smaller, gray circles show slip-rate sites on the Mill Creek strand of the San Andreas fault. Inset map of California shows location of Figure 1. AW—Ash Wash (Blisniuk et al., 2011); Az1—Anza (Rockwell et al., 1990); Az2—Anza (Blisniuk et al., 2011); BB—"Big Bend" in the San Andreas fault; BC—Badger Canyon (McGill et al., 2010); BF—Burro Flats (Orozco, 2004; Orozco and Yule, 2003; Yule and Spotila, 2010; see also Yule, 2009); BP—Biskra Palms (Behr et al., 2010; Fletcher et al., 2010; see also van der Woerd et al., 2006; Keller et al., 1982); Cb—Cabezon (Yule et al., 2001); CC—Cajon Creek (Weldon and Sieh, 1985); CHFZ—Crafton Hills fault zone; Cl—Calico fault (Oskin et al., 2008); Co—Colton (Wesnousky et al., 1991); CR—Camprock fault (Oskin et al., 2008); Cy—City Creek (1.2 mm/yr; Sieh et al., 1994); GT—Grand Terrace (Prentice et al., 1986); HF—Helendale fault (Oskin et al., 2008); LC—Lytle Creek (Mezger and Weldon, 1983); Ln—Lenwood fault (Oskin et al., 2008); LR—Littlerock (Weldon et al., 2008; Matmon et al., 2005); Lu—Ludlow fault (Oskin et al., 2008); NSTB—Northern San Timoteo Badlands (Morton et al., 1986; recalculated using new date in Morton and Matti, 1993, p. 224; Morton and Matti, 1993; Kendrick et al., 2002); Pa—Pallett Creek (Salyards et al., 1992); PF—Pisgah fault (Oskin et al., 2008); Pl—Plunge Creek (this paper); Pt—Pitman Canyon (McGill et al., 2010); RH—Rockhouse Canyon (Blisniuk et al., 2010); SA—Santa Ana River (2 mm/yr; R. Weldon, 2010); San Bdno—San Bernardino; SG Pass (and SGP, in inset)—San Gorgonio Pass; SSR—southern Santa Rosa Mountains (Blisniuk et al., 2010); Wa—Wallace Creek (Sieh and Jahns, 1984); WC—Wilson Creek (Harden and Matti, 1989).

Mountains), and (4) left-lateral faults of the Eastern Transverse Ranges (Fig. 1).

Differences in the plate-boundary configuration between central and Southern California sections of the San Andreas fault zone invite questions about the way in which 35 mm/yr of Holocene slip (Sieh and Jahns, 1984) on the Carrizo Plain section (north of the Big Bend) projects into Southern California. Investigations along the Mojave Desert segment of the San Andreas fault have shown that late Quaternary slip there is comparable to slip on the Carrizo segment (~35 mm/yr; Humphreys and Weldon, 1994; Salyards et al., 1992; Weldon et al., 1993, 2008; Schwartz and Weldon, 1986; Weldon, 1986; Matmon et al., 2005). However, in the Cajon Pass region (CC in Fig. 1), Weldon and Sieh (1985) found that—for the period between 6 ka and 14.4 ka—latest Pleistocene and Holocene rates on the San Andreas fault average ~24.5 ± 3.5 mm/yr. To reconcile this 10 mm/yr discrepancy, Weldon and Sieh (1985) proposed that the 35 mm/yr rate north of Cajon Pass is partitioned south of the pass into ~25 mm/yr

Downloaded from gsabulletin.gsapubs.org on January 7, 2013

on the San Andreas fault and ~10 mm/yr on the San Jacinto fault. This interpretation was supported by less-well-constrained rate determinations farther south along the San Andreas fault, including 14–25 mm/yr at Wilson Creek (Harden and Matti, 1989) and 10–35 mm/yr at Biskra Palms Oasis (Keller et al., 1982), and by well-constrained estimates over multiple latest Quaternary time scales of ~12 mm/yr (range 7–21 mm/yr) on the central San Jacinto fault near Anza (Rockwell et al., 1990; Sharp, 1981). Thus, within the southern San Andreas fault system, a 25 mm/10 mm split between the San Andreas and San Jacinto faults has been a traditional paradigm for evaluating paleoseismic results and attendant seismic potential.

A significantly different paradigm for Quaternary strain distribution within the southern San Andreas fault system allocates *less* slip on the San Andreas fault between Cajon Pass and the Coachella Valley and considerably *more* slip on the San Jacinto fault. In the San Gorgonio Pass region, field relations led Matti et al. (1985, 1992) and Matti and Morton (1993) to propose that dextral slip on the Coachella Valley segment of the San Andreas fault zone (Mission Creek strand) diminished in the early Quaternary with initiation of the San Gorgonio Pass knot in the San Andreas fault; as a consequence, dextral slip may have been largely accommodated on the newly evolving San Jacinto fault for some time. Stratigraphic relations within early Quaternary sedimentary rocks suggest that the northern San Jacinto fault initiated around 1.5 Ma (Morton et al., 1986; Morton and Matti, 1993). Other studies suggest more recent initiation (1.1–1.2 Ma) for the San Jacinto fault (Matti et al., 1985, 1992; Matti and Morton, 1993, their fig. 7I; Kirby et al., 2007; Lutz et al., 2006; Janecke et al., 2010). In combination with total bedrock offsets of ~20 km (Janecke et al., 2010) to ~25 km (Sharp, 1967), these fault initiation ages suggest that long-term slip on the San Jacinto fault ranges from ~17 (Morton and Matti, 1993) to ~20 mm/yr (Janecke et al., 2010). A few estimates of high slip rates (~20 mm/yr or more) over more recent time periods (50–100 ka) have been reported for the northern San Jacinto fault by Morton and Matti (1993) and Kendrick et al. (2002).

Thus, two major paradigms have arisen for the way in which dextral strain has been distributed within the southern San Andreas fault system between Cajon Pass and the Coachella Valley during the Quaternary: (1) partitioning of 25 mm/yr on the San Andreas fault and ~10 mm/yr on the San Jacinto fault, versus (2) partitioning of latest Quaternary slip rates more equally between the two faults or perhaps with even higher rates on the San Jacinto fault than on the San Andreas. These two paradigms provide a context for our latest Quaternary slip-rate estimates for the San Bernardino strand of the San Andreas fault in the Plunge Creek area, as well as for other recently estimated rates elsewhere along the southern San Andreas fault at Pitman Canyon and Badger Canyon (McGill et al., 2010), in San Gorgonio Pass (Orozco, 2004; Orozco and Yule, 2003; Yule and Spotila, 2010; Yule, 2009), and at Biskra Palms Oasis (van der Woerd et al., 2006; Behr et al., 2010; Fletcher et al., 2010). This paper will show that, for the last 35 k.y. or so, rates at Plunge Creek are inconsistent with the traditional 25 mm/10 mm split between the San Andreas and San Jacinto faults and suggest instead that the San Bernardino section of the San Andreas fault slips at a rate of 7–16 mm/yr, which is comparable to or less than that of the San Jacinto fault.

Aside from debates about the precise rate of slip on the San Jacinto fault, the locus and mechanism of slip transfer from the northern end of the San Jacinto fault onto the Mojave section of the San Andreas fault have also been matters of ongoing investigation. In the southeastern San Gabriel Mountains, a surface connection between the San Jacinto and San Andreas faults cannot be demonstrated (Morton, 1975; Morton and Matti, 1987). Given this constraint, Matti et al. (1985, 1992) reasoned that the low-lying San Bernardino Valley is a foundered extensional domain within a zone of right-stepping slip from the San Jacinto to the San Andreas fault. Others have proposed that rotations of blocks bounded by left-lateral faults buried beneath San Bernardino Valley may help to accommodate slip transfer across the valley (Nicholson et al., 1986; Seeber and Armbruster, 1995). Although the model of Matti et al. (1985, 1992; Matti and Morton, 1993) included the entire San Bernardino Valley within the stepover, more recent geophysical studies (Anderson et al., 2004) indicate that the right step occurs mainly in the west and northwest parts of San Bernardino Valley, with only ancillary effects in eastern parts of the stepover (for example, the Crafton Hills horst-and-graben complex and the Yucaipa Valley fault zone of Matti et al., 1985, 1992).

Present-Day Strain Rates: Geodetic Evidence

Interestingly, strain rates based on Quaternary geologic evidence are not everywhere compatible with real-time strain rates determined from global positioning system (GPS) and other geodetic techniques (Thatcher, 2009). South of San Gorgonio Pass, most geodetic studies suggest a co-equal or slightly larger role for the San Andreas fault (16–25 mm/yr) than for the San Jacinto fault (12–21 mm/yr) (Meade and Hager, 2005; Becker et al., 2005; Fay and Humphreys, 2005; Fialko, 2006; Spinler et al., 2010; Loveless and Meade, 2011), although one study using a viscoelastic rheology inferred greater slip on the San Jacinto fault (24–26 mm/yr) than on the San Andreas fault (16–18 mm/yr) (Lundgren et al., 2009).

In contrast, elastic models of geodetic data generally suggest a much reduced role for the San Andreas fault in the San Bernardino Valley and San Gorgonio Pass (Meade and Hager, 2005; Becker et al., 2005; Spinler et al., 2010). A substantial portion of the elastic strain across the Coachella Valley section of the San Andreas fault passes northward to the Eastern California shear zone (13–18 mm/yr according to Spinler et al., 2010), rather than remaining on the San Andreas fault. Likewise, a substantial portion of the elastic strain across the Mojave section of the San Andreas fault appears, in these models, to extend southward onto the San Jacinto fault, leaving a very low strain accumulation rate on the San Bernardino section of the fault (e.g., 5.1 ± 1.5 mm/yr—Meade and Hager, 2005; –2.3 ± 1.5 mm/yr—Becker et al., 2005; 5–8 mm/yr—Spinler et al., 2010; 8.2–10.5 mm/yr—Loveless and Meade, 2011). One study that suggested a higher strain accumulation rate across this part of the San Andreas fault (14.3 mm/yr; McCaffrey, 2005) did so only as a result of including geologic slip-rate data (using rates of 18–30 mm/yr for this section of the fault) in the same inversion with the geodetic data.

Low rates of elastic strain accumulation (<10 mm/yr) across the San Bernardino and San Gorgonio Pass sections of the San Andreas fault contrast dramatically with previously published Holocene and late Pleistocene slip-rate estimates (24.5 ± 3.5 mm/yr—Weldon and Sieh, 1985; 14–25 mm/yr—Harden and Matti, 1989), which are 3–5 times faster than rates inferred from modeling of geodetic data. Holocene and latest Pleistocene slip rates, averaged over the past few tens of thousands of years, justifiably have been a primary focus of seismic hazard studies, given that (1) this time scale is long enough to average out the effects of potentially irregular earthquake recurrence intervals, but (2) it is short enough to minimize the effects of changing tectonic regimes over longer time scales. For many faults worldwide, the present-day elastic strain accumulation rates are consistent with Holocene and latest Pleistocene slip rates (for example, compare Sieh and Jahns [1984] to Prescott et al. [2001]). However, for the San Bernardino and San Gorgonio Pass sections of the San Andreas fault, present-day elastic strain accumulation at relatively low rates (see previous references) does not appear

Downloaded from gsabulletin.gsapubs.org on January 7, 2013

to be compatible with previously published geology-based strain rates estimated for the latest Quaternary (Weldon and Sieh, 1985; Harden and Matti, 1989). The disparity between model-based estimates and geology-based estimates needs to be resolved in order for either barometer of late Quaternary strain to be used for seismic hazard analysis.

Focus of Our Investigation

In an effort to better understand potential spatial and temporal variations in the San Andreas fault slip rate between Cajon Pass and San Gorgonio Pass, we determined the latest Pleistocene slip rates at Plunge Creek, along the San Bernardino section of the San Andreas fault (Figs. 1 and 2). We estimate slip rates for two different latest Quaternary time periods. First, an erosional landform on the southwestern side of the fault (Fig. 3) is probably an ancient channel wall of Plunge Creek that has been right-laterally separated by ~290 m from a correlative terrace rise on the northeast side of the fault (Figs. 4 and 5). Second, a small, fine-grained alluvial fan is offset 130 ± 70 m from its most likely source gullies on the opposite side of the fault (Figs. 4 and 6).

METHODS

Geologic Mapping

Geologic mapping (Fig. 4) was conducted at scales ranging from 1:6000 to 1:2500, using as a base the 1995 digital aerial ortho-photo quarter quadrangle of the Redlands 7.5′ quadrangle obtained from the National Aerial Photography Program (U.S. Geological Survey–Earth Resources Observation and Science Center) available from Cal-Atlas Geospatial Clearing House (http://atlas.ca.gov/). Other mapping resources included stereo aerial photography (1983, U.S. Department of Agriculture [USDA], 1:14,000 scale; 1971, I.K. Curtis, 1:6300 scale; and 1938, unknown source, 1:20,000 scale) and 0.5 m resolution light detection and ranging (LiDAR) imagery from the B4 project (Bevis et al., 2005). We used the 1983, 1971, and 1938 aerial photographs to reconstruct geomorphic surfaces and alluvial deposits in areas where urbanization has obscured geological and geomorphic features.

Geologic mapping by the U.S. Geological Survey (USGS) in the San Bernardino Valley region has led to a regional classification of surficial units (e.g., the Redlands and Yucaipa 7.5′ quadrangles; Matti et al., 2003a, 2003b). We use this classification approach in our investigation, although we have revised map-unit assignments in the Plunge Creek area based on our detailed mapping and geochronologic data (compare with Matti et al., 2003b). Consistent with Matti et al. (2003a, 2003b), we use Qo3 designations for late Pleistocene units, Qy1 for latest Pleistocene to early Holocene units, and Qy2, Qy3, Qy4, and Qy5 for progressively younger deposits. Wash deposits within confined channels are designated with "w" (e.g., Qyw1), fan deposits with "f" (e.g., Qyf2), alluvium that does not readily fit either of these categories with "a" (e.g., Qya2), and colluvium with "c" (e.g., Qyc1).

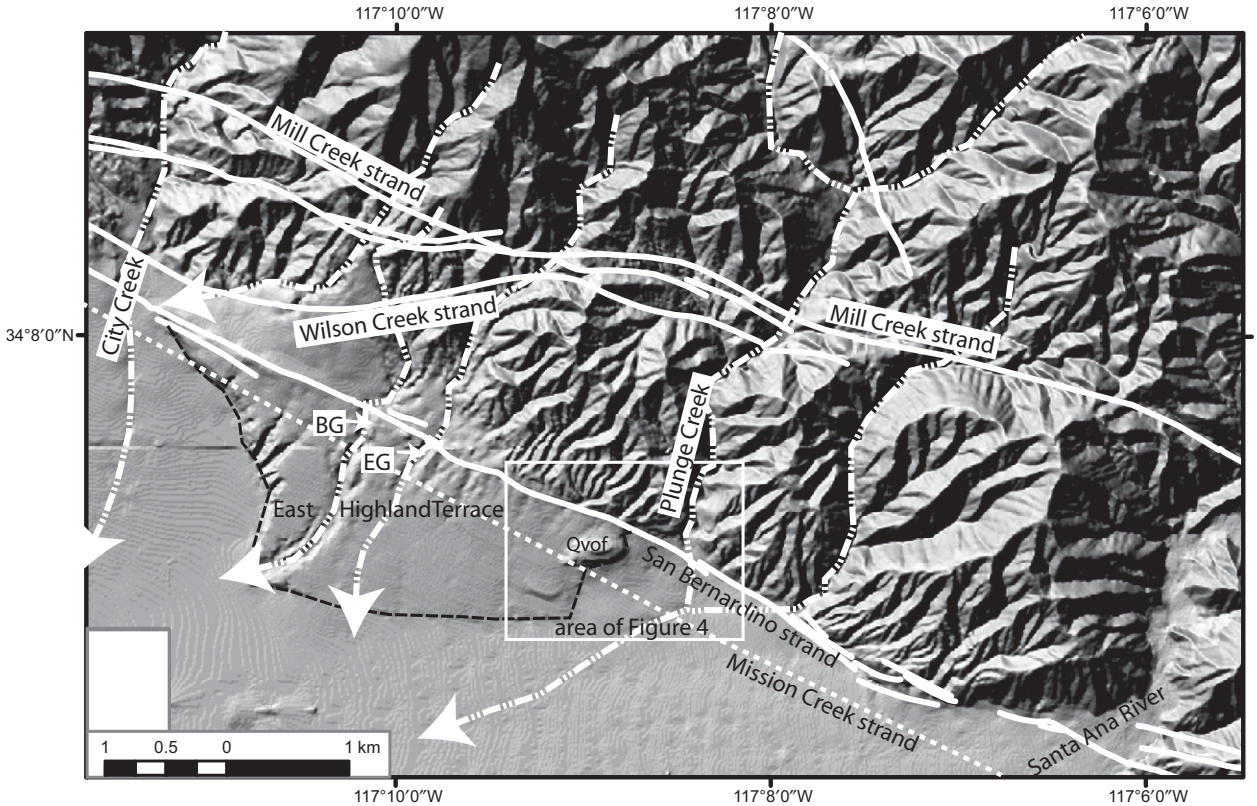

Figure 2. Digital elevation model (with 10 m resolution, from the U.S. Geological Survey, national elevation data set) showing location of the Plunge Creek slip-rate site (box labeled "area of Fig. 4") relative to San Andreas fault strands (thick white lines), major drainages (thin white lines with dash-dot pattern), and high-standing Pleistocene alluvial-fan deposits (East Highland Terrace). BG—Bledsoe Gulch; EG—Elder Gulch; Qvof—knob of very old alluvium discussed in text. Inferred location of the buried Mission Creek strand is from Matti et al. (2003b). Other fault locations are from the U.S. Geological Survey and California Geological Survey (2006).

Downloaded from gsabulletin.gsapubs.org on January 7, 2013

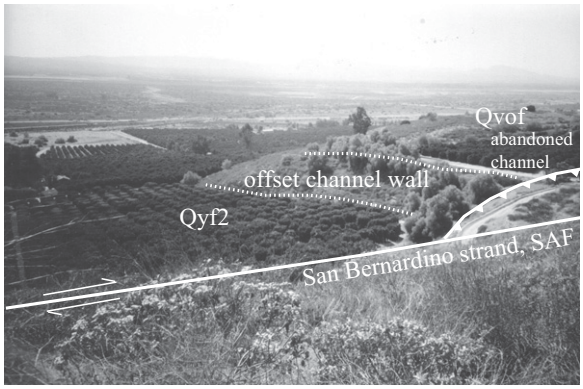

Figure 3. View of offset channel wall, incised into southeast side of the Qvof knob on southwest side of fault. We correlate this offset channel wall with the Qow3b/Qyw1 riser on the northeast side of the fault. Photograph was taken 25 October 1996, prior to grading and development of the site. View to west from a point northeast of the fault, at the yellow star in Figure 5. SAF—San Andreas fault. Scale of photo is indicated by trees within the orange grove beneath the Qyf2 label.

Profiles, Excavations, and Dating

Profiles and cross sections (see Fig. 4 for locations) were constructed to portray relationships among units, to evaluate possible cross-fault correlations, and to measure vertical offsets. To clarify stratigraphic, lithologic, and temporal relations among key Quaternary units and to collect samples for dating these units, we (1) excavated trenches and cuts (one-sided excavations to enhance natural exposures), (2) took advantage of cuts excavated during grading of the site for development, and (3) examined logs of trenches excavated by previous investigators. Eighteen detrital charcoal samples were collected and dated for this study (Table 1).

Samples for optically stimulated luminescence (OSL) dating were collected by hammering opaque plastic or steel tubes, ~20 cm long, into freshly cleaned natural exposures. The tubes were sealed and placed in light-proof photographic bags pending the initial processing at the University of Cincinnati. Laboratory preparation followed methods described in Seong et al. (2007). Luminescence signals were measured using a Risø TL/OSL reader (model DA-20). Luminescence from quartz grains was stimulated using an array of blue light-emitting diodes (470 nm, 50 mW/cm^2) filtered using a green long-pass GG-420 filter. Detection was through a Hoya U-340 filter. All quartz aliquots were screened for feldspar contamination using infrared stimulation with infrared light-emitting diodes (870 nm, 150 mW/cm^2). All OSL signals were detected using a 52-mm-diameter photomultiplier tube (9235B). The equivalent dose (De) measurements were determined on multiple aliquots using the single aliquot regenerative (SAR) method protocol developed by Murray and Wintle (2000). Growth-curve data were fitted using linear and exponential trend curves. The De value for every aliquot was examined using Risø Analysis 3.22b software. Aliquots with poor recuperation (>10%) were not used in the age calculations. For each sample, equivalent doses of all aliquots were averaged and then divided by the dose rate, giving a mean age (Table 2). Calculation uncertainties and methods used to calculate dose rates are explained in the footnotes in Table 2.

Soil development was described for a pedon associated with Qyc1. Field properties, including color, texture, structure, dry and wet consistence, and clay films, were measured (Soil Survey Staff, 2010; Birkeland, 1999). A profile development index was determined, using rubification, texture, clay films, and dry consistence (Harden, 1982; Harden and Taylor, 1983).

GEOLOGY OF THE PLUNGE CREEK STUDY AREA

Faults

The Plunge Creek slip-rate site is located about midway along the length of the San Bernardino section of the San Andreas fault zone (Fig. 1). Within this region, there are four major strands of the San Andreas zone. Of these, the San Bernardino strand represents the modern trace of the fault and has the greatest Holocene activity (Matti and Morton, 1993; Sieh et al., 1994); this fault is shown by a thick black line in Figure 1. Our study estimates the slip rate across this strand where it crosses Plunge Creek at ~34.177°N, 117.141°W (Figs. 1 and 2). Matti and Morton (1993) suggested that the San Bernardino strand has only 3 km of total offset. The Mission Creek strand probably has 89 km of total offset and, at the location of Plunge Creek, is inferred to be concealed beneath alluvium slightly valley-ward from the San Bernardino strand (Fig. 2; Matti and Morton, 1993; Matti et al., 2003b). Two other strands of the San Andreas fault zone cross Plunge Creek ~2 km north of the San Bernardino strand (Fig. 2). These are the Wilson Creek strand and the Mill Creek strand, which appear to have 40 km and 8 km of cumulative offset, respectively (Matti and Morton, 1993).

Of this family of dextral faults, only the San Bernardino and the Mill Creek strands have been active in the latest Quaternary, with the majority of slip during this period accommodated by the San Bernardino strand (Matti and

Figure 4 (*on following page*). Geologic map of the Plunge Creek site showing locations of excavations and piercing points that constrain offset estimates for dextral slip. Squares and circles indicate piercing points on the southwest and northeast sides of the fault, respectively. Yellow symbols indicate piercing points for the ca. 10.5 ka Qyf2 fan (see Fig. 6 for greater detail). Light-blue symbols indicate piercing points for the ca. 35 ka Qow3b/Qyw1 riser and its correlative channel wall on the southwest side of the fault (see Fig. 5 for greater detail). Symbols with solid outline are the preferred piercing points; those with dashed outline indicate points used to estimate maximum and minimum limiting offsets. T1, T2, T3, and C5 are excavations conducted solely for the purpose of this study. For cross sections along these excavations, see Figures 8 and 9 and Data Repository sheets DR2 and DR1 (see text footnote 1), respectively. L217, L219, L220, L44–52, and lot W indicate construction cuts (on lots 217, 219, 220, 44–52, and W, respectively) that were examined for this study. For photomosaics showing these exposures, see Figure 10 (lots 217–220) and Data Repository sheets DR3 (lots 44–52) and DR6 (lot W) (see text footnote 1). R1–90, R1–99, R27 and 27A, S1, S3, S4, P1, P2, P3, and P6 are prior excavations discussed in the text. See Data Repository sheet DR4 for the log of the south end of R1–99 and sheet DR5 for logs of S1, S3, and S4 (see text footnote 1). Cross-section A-A′ is illustrated in Figure 7; topographic profiles B-B′ and C-C′ are illustrated in Figure 12, and profile E-E′ is shown in Figure 9. Contours were constructed using ESRI's ArcGIS software from a 10 m digital elevation model from the U.S. Geological Survey, national elevation data set. This area has been mapped at a smaller scale by Matti et al. (2003b). To avoid clutter, the location of the buried Mission Creek strand of the San Andreas fault (SAF) is not shown here, but it is shown approximately in Figure 2.

Downloaded from gsabulletin.gsapubs.org on January 7, 2013

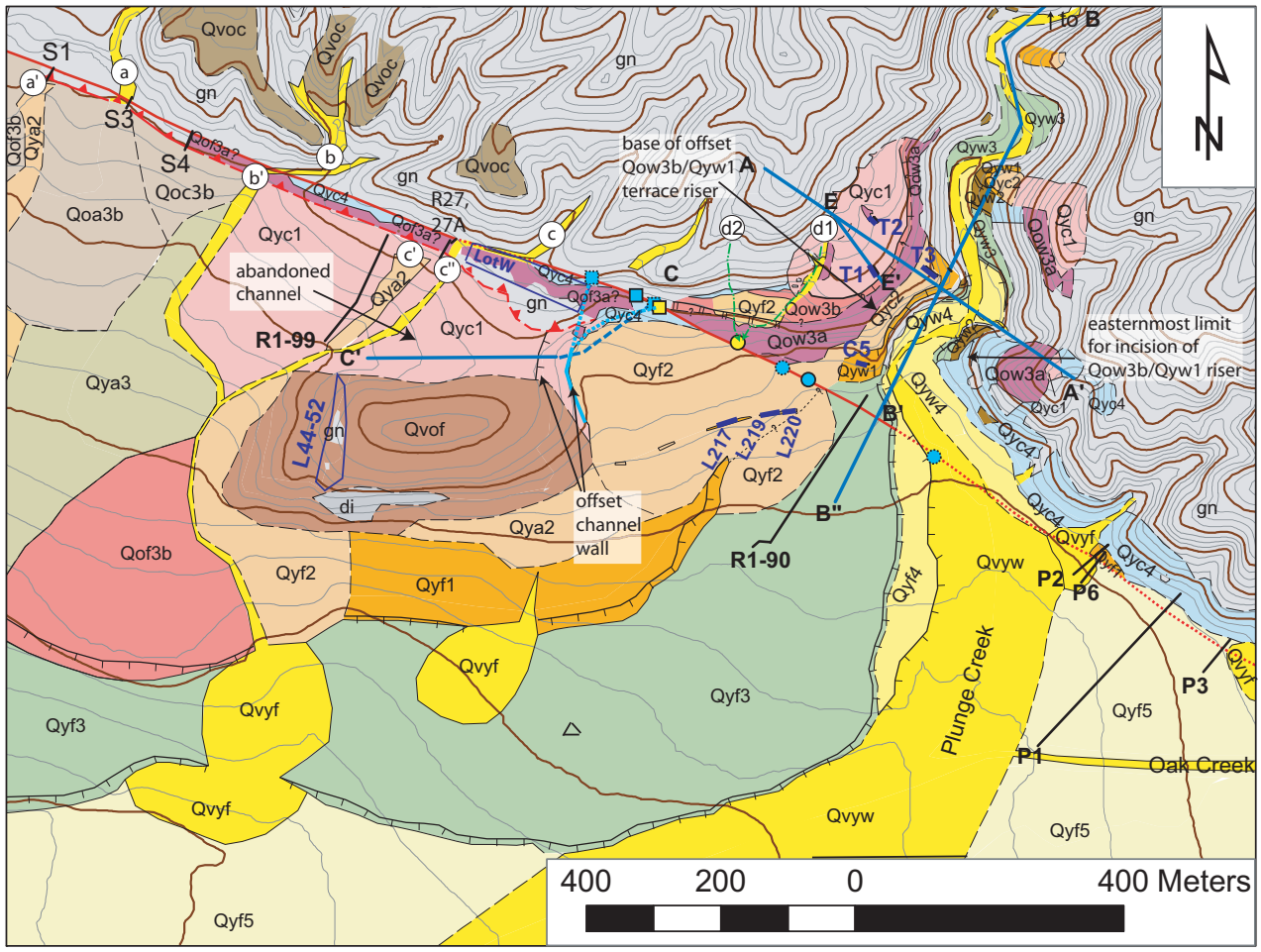

Piercing points
- Qow3/Qyw1riser
- Qya2 fan apex and source
- (a) other drainages

Other features
- profile lines
- projection of selected offset features to fault
- excavations (this study) (T1, T2, T3, C5, L217, L218, L220)
- excavations (previous studies) (R1-90, R1-99, P1, P2, P3, P6, S1, S3, S4)
- 20-m topographic contour
- 5-m topographic contour

Contacts
- top of riser
- contact
- contact, approximate
- contact, uncertain
- inferred contact, concealed

Faults
- fault
- fault, buried — San Bernardino strand, SAF
- reverse fault, queried where inferred

Coarse-grained alluvium		Fine-grained alluvium and colluvium
Qvyw, Qvyf	Holocene	Qyc4
Qya5		Qya3
Qya4		Qyc2, Qyf2, Qya2
Qyw3, Qyf3		Qyc1
Qyw2		Qoa3b, Qoc3b
Qyw1, Qyf1	Late Pleistocene	
Qow3b, Qof3b		
Qow3a, Qof3a		
Qvof	Middle Pleistocene	Qvoc

Basement rock
- di — diorite
- gn — gneiss
- of Wilson Creek block (Matti and Morton, 1993)

Figure 4.

Downloaded from gsabulletin.gsapubs.org on January 7, 2013

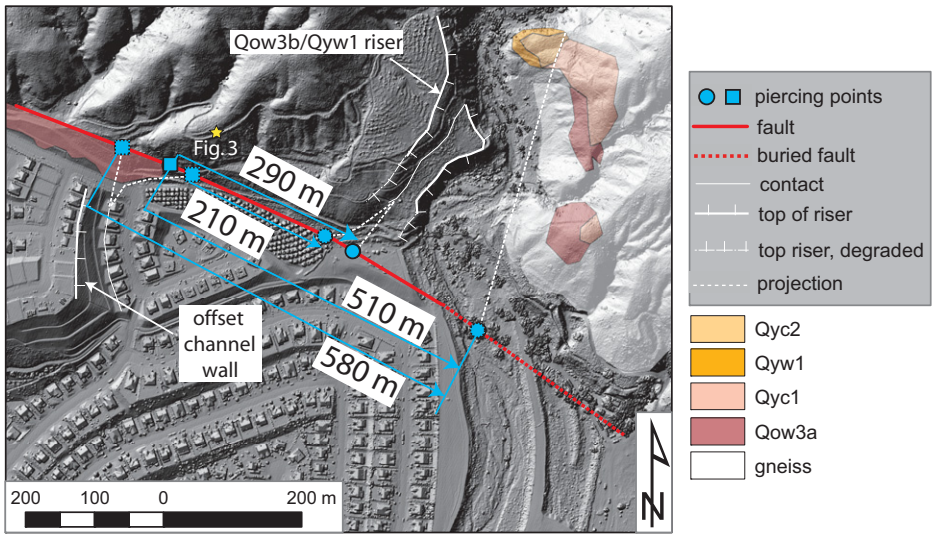

Figure 5. B4 light detection and ranging (LiDAR) image of the Plunge Creek site showing features used to measure the offset of the Qow3b/Qyw1 riser from the offset channel wall, since the time of initial incision ca. 35 ka. Blue squares and circles indicate piercing points on the southwest and northeast sides of the fault, respectively. The piercing points corresponding to the preferred offset have a solid outline; those corresponding to alternative offsets have a dashed outline. Selected geologic units on the southeast side of Plunge Creek are shown to constrain the easternmost limit at which the initial incision of the Qow3b/Qyw1 riser could have occurred. Yellow star shows approximate location from which the photograph in Figure 3 was taken.

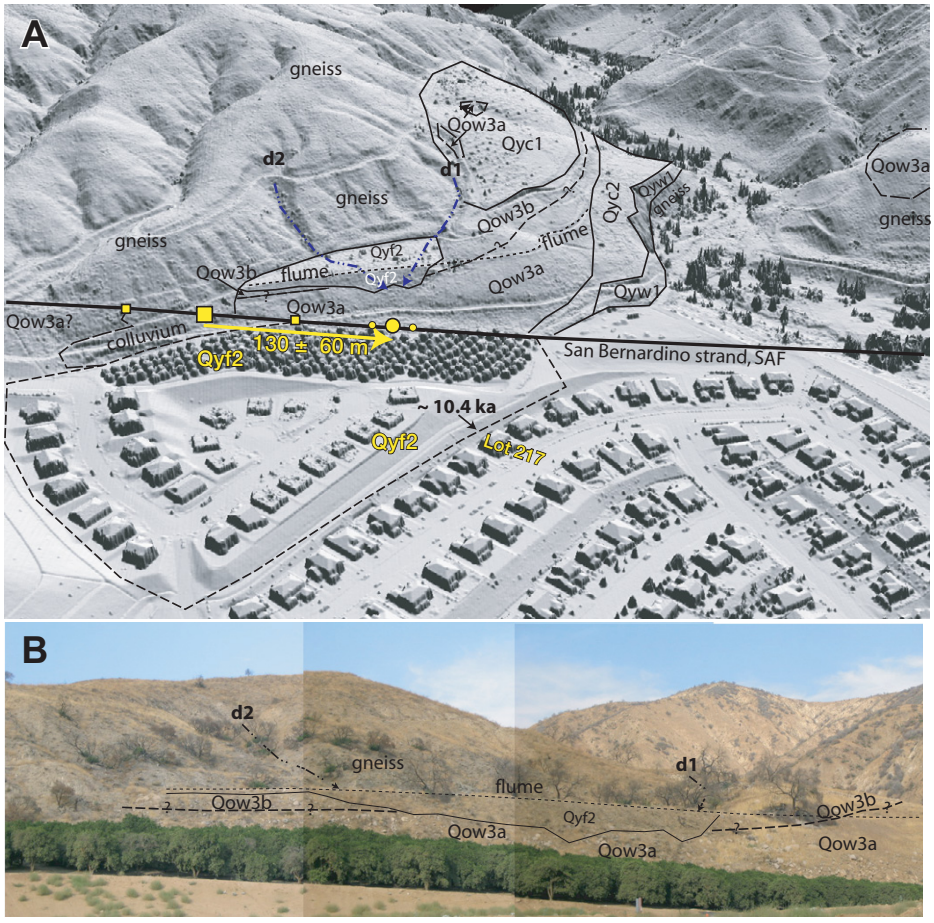

Figure 6. (A) B4 light detection and ranging (LiDAR) image showing broad apex of the Qyf2 fan offset from source gullies d1 and d2, which are buried by late-stage Qyf2 fill near the fault. Large, yellow square shows center of the broad apex, and smaller squares show edges of the apex. See also Figure 4, where topographic contours display the broad apex. Yellow circles show piercing points on the northeast side of fault, showing the range of possible projections of gullies d1 and d2 to the fault. The location and average age of two dated samples from Qyf2 within a construction cut in housing Lot 217 are also shown (See Fig. 10 for greater detail). (B) Photomosaic of same area showing fine-grained Qyf2 (lacking boulders) overlying the bouldery deposits of Qow3a and Qow3b. San Bernardino strand is located behind the trees at the base of the slope on which Qyf2 and Qow3a/3b are exposed. Contact between Qow3a and Qow3b is not visible in the field but is inferred, as explained in section "Qow3b: Veneer of reworked fluvial deposits on a cut terrace incised into Qow3a." Scale of photo is indicated by trees in orange grove in foreground. SAF—San Andreas fault.

Downloaded from gsabulletin.gsapubs.org on January 7, 2013

TABLE 1. RADIOCARBON DATES FROM THE PLUNGE CREEK SITE

Lab no.	Sample name	$\delta^{13}C$* (‰)	Fraction modern	±	$\delta^{14}C$ (‰)	±	^{14}C age† (yr)	± (yr)	Calibrated age§ Mean (yr B.P.)	2σ range (yr B.P.)	Context
130977	PCSR-7 split 1	–24.66	0.8504	0.003	–149.6	3	1300	30	1240	1177–1289	From colluvium burying the abandoned channel
119558	PCSR-T3-8	–23.8	0.3982	0.0015	–601.8	1.5	7395	35	8241	8071–8335	From low terrace colluvuim (Qyc2)
130971	PCSR-T3-9	–24.09	0.3993	0.0014	–600.7	1.4	7375	30	8212	8053–8321	From low-terrace colluvium (Qyc2)
131470	PCSR-T3-11	–27.52	0.3446	0.0012	–655.4	1.2	8560	30	9535	9495–9551	From low terrace colluvium (Qyc2)
130972	PCSR-8	–25.38	0.3113	0.0012	–688.7	1.2	9375	35	10610	10,512–10,697	Qyf2, about 1 m above top of Qyf1 gravel
130973	PCSR-18	–25.37	0.2616	0.001	–738.4	1	10770	30	12664	12,573–12,762	Qyf1, lot 220
130974	PCSR-1	–25	0.3156	0.0027	–684.4	2.7	9260	70	10438	10,249–10,647	Qyf1, lot 219
130976	PCSR-C5-7b	–25	1.0935	0.0042	93.5	4.2	Modern				Low terrace gravel in cut 5 (Qyw1)
AA18422	PC2-1	–25.7					9180	100	10382	10,186–10,647	Pebbly gravel in T2 at paleoseismic site (Qyf1?)
AA27511	PC-6E-57	–24.7					11330	85	13217	12,984–13,406	Pebbly gravel in T6 at paleoseismic site (Qyf1?)
AA18419	PC1-4	–24.9					18820	190	22518	22,025–23,296	Sandy colluvium(?) in T1 at paleoseismic site
AA18418	PC1-1	–22.4					22590	310	27258	26,281–28,025	Sandy colluvium(?) in T1 at paleoseismic site
119554	PCSR-T1-10	–25.6	0.9556	0.0031	–44.4	3.1	365	30	416	316–502	High terrace colluvium (Qoc2)
119555	PCSR-T1-11	–25	1.0842	0.0058	84.2	5.8	Modern				High terrace colluvium (Qoc2)
130975	PCSR-T1-2	–22.2	0.0282	0.0007	–971.8	0.7	28650	190	33093	32,169–33,981	High terrace colluvium, within basal contact zone
119553	PCSR-T1-3	–25.1	0.0201	0.0004	–979.9	0.4	31380	180	35833	35,211–36,461	Base of high terrace colluvium (Qoc2)
119557	PCSR-T2-8	–23.6	0.0244	0.0016	–975.6	1.6	29840	520	34396	33,176–35,156	High terrace colluvium (Qoc2)
119556	PCSR-T2-1	–25	0.0108	0.0066	–989.2	6.6	36400	4900		>35,632	High terrace colluvium (Qoc2)

Note: Most samples were dated at the Center for Accelerator Mass Spectrometry, Lawrence Livermore National Laboratory, except for those with an AA prefix in the laboratory number, which were dated at the National Science Foundation–University of Arizona facility.

*$\delta^{13}C$ values that are given with a single decimal place were measured. Values given without decimal places are the assumed values according to Stuiver and Polach (1977, p. 355).

†The quoted age is in radiocarbon years using the Libby half-life of 5568 yr and following the conventions of Stuiver and Polach (1977).

§Radiocarbon ages were calibrated with OxCal 4.1 (Bronk Ramsey, 2009) using calibration curve IntCal09 (Reimer et al., 2009).

TABLE 2. OPTICALLY STIMULATED LUMINESCENCE DATA AND DATING RESULTS

Sample number	Trench number: geologic unit	Altitude (m asl)	Depth (cm)	Particle size (μm)	U* (ppm)	Th* (ppm)	K* (%)	Rb* (ppm)	Cosmic†,§ (G/k.y.)	Dose rate†,# (G/k.y.)	*n***	Mean equivalent dose†† (Gy)	OSL age§§ (ka)
PCSR02	Lot 217: Qyf1	490	200	90–125	1.90	11.5	3.54	158	0.15 ± 0.02	4.73 ± 0.24	17(24)	73.4 ± 15.1	11.5 ± 0.7
PCSR03	Lot 217:Qyf2	490	120	90–125	2.40	29.3	3.44	132	0.17 ± 0.03	5.98 ± 0.35	23(24)	73.4 ± 15.1	10.2 ± 0.7
PCSR04	Lot 44:Qvof	500	600	90–125	2.10	13.6	3.60	158	0.08 ± 0.02	4.91 ± 0.25	(24)	Saturated	–
PCSR06	T1:Qyc1	537	278	90–125	2.48	22.3	2.19	141	0.17 ± 0.02	4.04 ± 0.24	12(30)	80.5 ± 13.9	19.9 ± 1.5
PCSR08	T2: Qyc1	545	266	125–180	1.84	23.0	2.11	120	0.17 ± 0.02	3.87 ± 0.23	19(30)	68.2 ± 17.2	17.6 ± 1.5
PCSR09	T2: Qyc1	545	354	180–250	1.77	36.7	2.08	107	0.15 ± 0.02	4.70 ± 0.28	37(43)	67.1 ± 22.5	14.3 ± 1.2
PCSR13	Cut 5: Qyw1	499	261	90–125	3.15	17.6	2.77	146	0.17 ± 0.02	4.37 ± 0.27	16(19)	61.6 ± 18.2	14.1 ± 1.4
PCSR14	Cut 5: Qyw1	499	255	90–125	3.73	23.4	2.8	156	0.17 ± 0.02	4.90 ± 0.29	14(30)	73.4 ± 15.1	15.0 ± 1.2

Note: OSL—optically stimulated luminescence.

*Elemental concentrations from neutron activation analysis of whole sediment measured at U.S. Geological Survey Nuclear Reactor Facility in Denver. Uncertainty taken as ±10%.

†Estimated fractional present-day water content is 10% ± 5%.

§Estimated contribution to dose rate from cosmic rays calculated according to Prescott and Hutton (1994). Uncertainty taken as ±10%.

#Total dose rate from beta, gamma, and cosmic components. Beta attenuation factors for U, Th, and K compositions incorporate grain-size factors from Mejdahl (1979). Beta attenuation factor for Rb is arbitrarily taken as 0.75 (cf. Adamiec and Aitken, 1998). Factors utilized to convert elemental concentrations to beta and gamma dose rates are from Adamiec and Aitken (1998) and beta and gamma components attenuated for moisture content.

**Number of replicated equivalent dose (D_E) estimates used to calculate mean D_E. The number in parenthesis is the total number of aliquots measured. These are based on recuperation error of <10%.

††Mean equivalent dose (D_E) determined from replicated single-aliquot regenerative-dose (SAR; Murray and Wintle, 2000) runs. Errors are 1σ, incorporating error from beta source estimated at about ±5%.

§§Errors incorporate dose-rate errors and 1σ standard errors (i.e., $\sigma_{n-1}/n^{1/2}$) for D_E.

Downloaded from gsabulletin.gsapubs.org on January 7, 2013

Morton, 1993; McGill et al., 1999). Sieh et al. (1994) suggested that the latest Quaternary slip rate for the Mill Creek strand is ~10% of the rate of the San Bernardino strand, and a latest Quaternary rate of 2 mm/yr has been estimated directly for the Mill Creek strand (R. Weldon, 2010). The Mill Creek strand is estimated to have begun activity in the middle Pleistocene and to have tapered in activity when the San Bernardino strand became active later in the Pleistocene (Matti and Morton, 1993).

Alluvial Stratigraphy and Geomorphology

We begin by describing geologic units on the northeast side of the San Bernardino strand. This is followed by a description of units on the southwest side of the fault and an explanation of our proposed correlations across the fault.

Units Northeast of the Fault

Qow3a: Major late Pleistocene canyon fill. Deposits of Qow3a fluvial gravel are present on both walls of Plunge Creek, constituting up to 30–40 m of clast-supported gravel, containing rounded, granitic boulders that commonly exceed 1 m in diameter. The top of the Qow3a deposits forms a major fill terrace, at elevations of 55–60 m above the modern channel. Just upstream from the San Bernardino strand, Qow3a deposits are clearly exposed on the east side of Plunge Creek (Fig. 4). On the west side of Plunge Creek, Qow3a (and Qow3b, see following) is exposed within a terrace riser that extends to a height of 48 m above the modern channel. Qow3a is also exposed at elevations up to 55–60 m above the modern channel along the southeast bank of gully d1 and within a small gully near T2, both of which have incised the thick colluvial wedge (Qyc1) that buries most of Qow3a (Fig. 4). We thus infer that Qow3a formed a >400-m-wide fan head where Plunge Creek crosses the San Bernardino strand.

We have no age control on Qow3a, except that it must be older than Qow3b (discussed later herein). We infer that Qow3a may be comparable in age to Weldon's (1986) Qoa-d, the most prominent late Pleistocene aggradational pulse in the Cajon Pass area. Weldon (1986) inferred Qoa-d to be 55 ka, based on its 1.3–1.4 km offset near Prospect Creek and the San Bernardino strand slip rate of 24.5 mm/yr at Cajon Creek (Weldon and Sieh, 1985). The age of Qoa-d may potentially be slightly older, given that the San Bernardino strand slip rate may decrease rapidly southeast of Cajon Creek and may be between 19 and 24 mm/yr at Prospect Creek (McGill et al., 2010). We consider 55–70 ka to be a reasonable estimate for the age of Qow3a. This is consistent with new dates presented in this paper for the younger unit, Qow3b.

Qow3b: Veneer of reworked fluvial deposits on a cut terrace incised into Qow3a. On the west side of Plunge Creek, a terrace riser above Qyw1 and Qyc2 (labeled "Qow3b/Qyw1 riser" in Figs. 4 and 7) exposes rounded granitic boulders that are likely part of the Qow3a fill. The top of the riser and of the boulder deposits is 48 m above the modern channel, i.e., somewhat lower than the 55–60 m height of the top of the other Qow3a deposits elsewhere. This suggests the presence of a cut terrace incised into Qow3a.

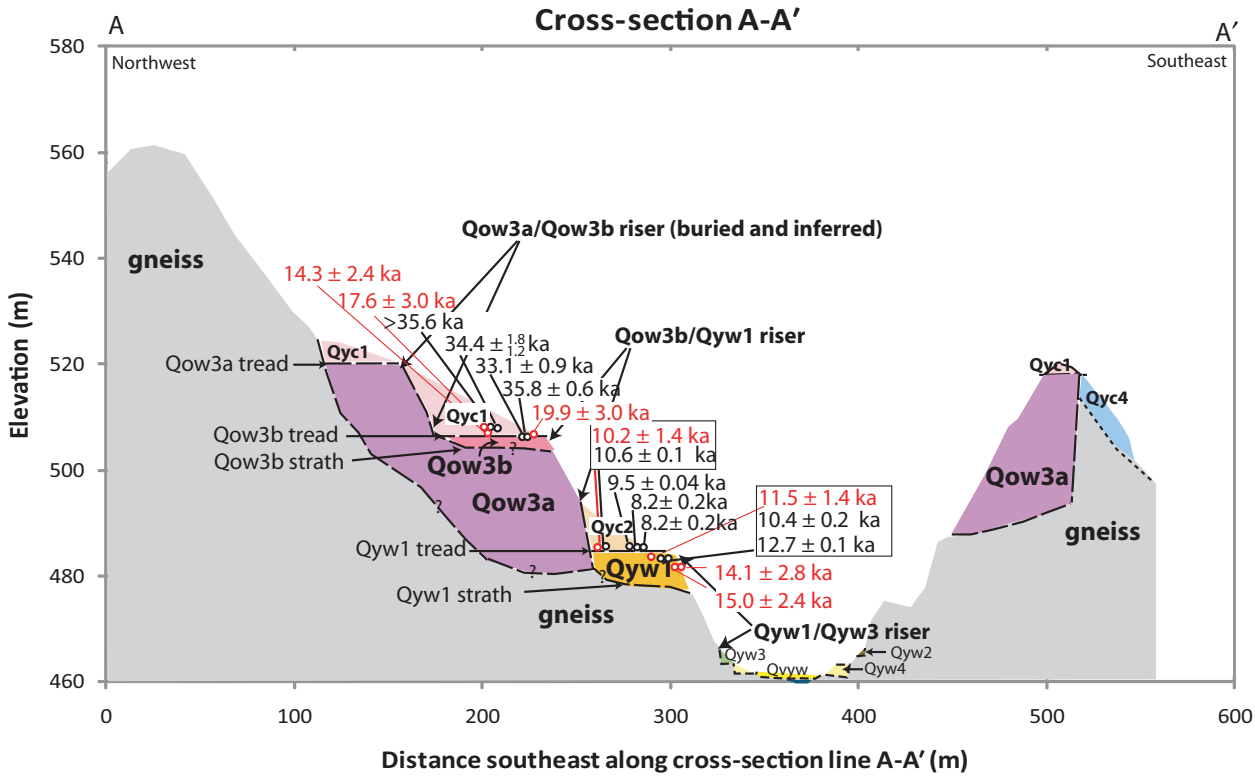

Figure 7. Cross-section A-A′ across Plunge Creek, northeast of the San Bernardino strand, showing fluvial terraces. The riser between Qow3b and Qyw1 is separated 290 m from the offset channel wall at the southeast edge of the Qvof knob on the opposite side of the fault. Calibrated radiocarbon dates are shown in black; optically stimulated luminescence (OSL) dates are in red. Reported errors are 2σ. Radiocarbon dates inside boxes are from the southwest side of the fault but are shown in their inferred stratigraphic positions. Note: Elevations are from the B4 LiDAR data (Bevis et al., 2005) and are ~30 m lower than elevations shown on U.S. Geological Survey topographic maps and on the 10 m digital elevation model that was used in Figure 4. Also note that the contact between Qow3b and Qow3a is not visible in the field, but is inferred, as explained in section "Qow3b: Veneer of reworked fluvial deposits on a cut terrace incised into Qow3a."

Downloaded from gsabulletin.gsapubs.org on January 7, 2013

The tread of this cut terrace is exposed where it intersects the top of the Qow3b/Qyw1 riser and is also exposed in trench 1, beneath a cover of Qyc1 colluvium (Figs. 8 and 9). Trench 2 exposes only colluvium (Qyc1), providing further support that the Qow3a gravel was incised to at least the base of trench 2.

The granitic boulder gravel exposed in the Qow3b/Qyw1 riser (Figs. 4 and 7) is probably mostly Qow3a, with a thin veneer of gravel remobilized as Qof3b just below the surface of the cut terrace. The degraded natural exposures and coarse nature of the deposits do not permit a contact to be recognized between Qow3b and Qow3a, so it is not possible for us to determine the thickness of Qow3b. In Figures 4 and 7, we represent Qow3b as being only a few meters thick. This is consistent with the relatively small size of the alluvial fan (Qof3b) southwest of the fault that we correlate with the Qow3b deposits (as justified in the upcoming section, "Qof3b: Late Pleistocene(?) fan and channel deposits from Plunge Creek, related to the 'abandoned channel'").

Just northeast of the San Bernardino strand, on the west side of Plunge Creek, granitic boulder gravel is exposed in the slope that rises to the northeast above the fault (in the vicinity of gullies d1 and d1 in Figs. 4 and 6). The top of this gravel is at an elevation that is roughly consistent with the elevation of the Qow3b terrace tread on the west bank of Plunge Creek, where that tread crops out at the top of the Qow3b/Qyw1 riser, ~48 m above Plunge Creek. This suggests that, during Qow3b time, Plunge Creek (and the tread of the Qow3b cut terrace) wrapped around the west bank of the canyon mouth within a channel that approached the San Bernardino strand at a low angle. This will be important later in the paper, when we reconstruct the channel of Plunge Creek across the San Bernardino strand during Qow3b time.

Qyc1: Late Pleistocene colluvial wedge. On the west side of Plunge Creek, both the Qow3a fill terrace and the lower terrace cut into it, with its inferred veneer of Qow3b deposits, are buried by a single, large wedge of colluvium (Qyc1) (Figs. 4 and 7). Qyc1 is composed of unstratified, unsorted silty sand, parts of which may have been homogenized by bioturbation, which, unfortunately, complicates the dating (see next section). We infer that buried beneath this colluvial wedge, there is a terrace riser that separates the tread of the Qow3a fill terrace from the strath of the Qow3b cut terrace. We refer to this riser as the Qow3a/Qow3b riser (Fig. 7). We estimate that the location of this riser is northwest of T2, which exposed only Qyc1 at an elevation where Qow3a would be expected, and southeast of the granitic boulders

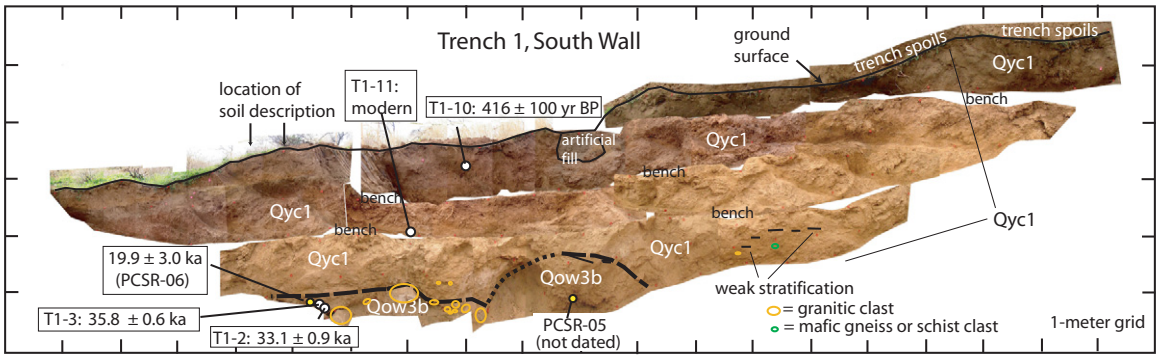

Figure 8. Photomosaic of south wall of trench 1, showing the toe of the Qyc1 colluvial wedge on top of Qow3b and locations of C-14 (white circles) and optically stimulated luminescence (OSL) (yellow circles) samples. For clarity, the "PCSR" prefix has been omitted from C-14 sample numbers on this figure.

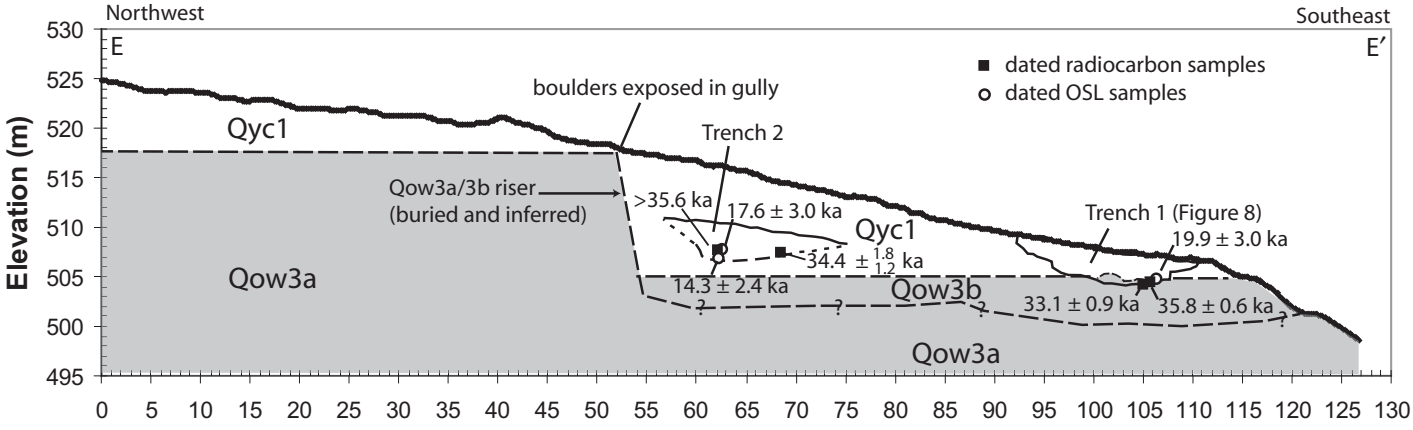

Figure 9. Profile E-E′ showing position of trenches 1 and 2 within the colluvial wedge (Qyc1) that buries the Qow3b terrace tread. Profile passes through trench 1 (see Fig. 4 for location). Location of trench 2 has been projected into the profile. Black squares indicate locations of radiocarbon dates; white circles indicate locations of optically stimulated luminescence (OSL) dates (ages in smaller font). Elevations are from the B4 light detection and ranging (LiDAR) data (Bevis et al., 2005) and are ~30 m lower than elevations shown on the Redlands U.S. Geological Survey topographic quadrangle.

Downloaded from gsabulletin.gsapubs.org on January 7, 2013

from Qow3a that crop out in gullies incised into Qyc1 (e.g., Fig. 9).

Age control for Qyc1. We have no direct dates that are unequivocally from Qow3a or Qow3b, but we do have several radiocarbon and OSL dates from near the base of the colluvium (Qyc1) that overlies Qow3b. We dated two detrital charcoal samples (T1–2, T1–3) and one OSL sample (PCSR-OSL-06) from near the contact between Qow3b and the overlying colluvium in trench 1 (Fig. 8). All three samples are from sandy material that may either be the matrix of Qow3b or the base of Qyc1. In either case, they should closely approximate the age of abandonment of Qow3b as a result of the initial incision of the terrace riser between Qow3b and Qyw1.

Trench 2 sampled deeper material, from within a thicker portion of Qyc1, closer to its source (Fig. 9). The trench was excavated into the base of a natural gully so that the top of the trench was ~4.5 m below the Qyc1 surface, and its base extended to a depth of 8–9 m below the surface of the deposit, potentially sampling an older part of this colluvial wedge than exposed in trench 1. Two detrital charcoal samples (T2–1 and T2–8) and two OSL samples (PCSR08 and PCSR09) were dated from near the base of trench 2. These samples are close to the terrace riser that is the source of Qyc1 and are only 2–2.5 m above the inferred top of Qow3b (Fig. 9). Thus, they probably postdate the abandonment of Qow3b relatively closely.

Three of the four radiocarbon dates from near the base of Qyc1 are in agreement and suggest a transition from Qow3b to Qyc1 deposition around 34.9 ka (Figs. 8 and 9; samples T1–2, T1–3, and T2–8 in Table 1). This value is the mean of the probability density function for these three dates combined (using the date combination tool in OxCal 4.1 [Bronk Ramsey, 2009]). A fourth radiocarbon date (sample T2–1) has a slightly older radiocarbon age that lies partially beyond the range of the calibration curve; however, its uncertainty is large enough to overlap with the other three dates (Table 1). Furthermore, it would not be unusual for an individual detrital charcoal sample to be older than others in a related population if it took a longer time to reach the deposit. In contrast to the radiocarbon dates, the three OSL dates from the same parts of Qyc1 are substantially younger, ranging in age from 14.3 to 19.9 ka (Figs. 8 and 9; samples PCSR06, 08, and 09 in Table 2).

We favor the radiocarbon dates from Qyc1 over the OSL dates for the following reasons. (1) The degree of soil development within Qyc1 supports an age of at least 35 ka, when compared to dated soils in the Cajon Pass chronosequence (Table 3). (2) Although there were no recognizable burrows near the OSL sample locations, Qyc1 is unstratified and may very well have been bioturbated, thereby intermixing multiple generations of sediment and biasing our OSL determinations. It is clear that some bioturbation did occur because a charcoal sample (T1–11) from 1.6 m beneath the surface of Qyc1 (and ~1.3 m above the 19.9 ± 1.5 ka OSL sample) has a modern age (Fig. 8). Bioturbation also is one possible explanation for the stratigraphic inversion of the 14.3 ± 1.2 ka and 17.6 ± 1.5 ka OSL samples from Qyc1 in trench 2, although the 2σ uncertainties do allow these two samples to be the same age. (3) By comparison with OSL determinations, the radiocarbon dates are more consistent. Three of the four samples from the base of Qyc1 are in close agreement, and the fourth, though older, is within the uncertainties. Of course, it is possible that all four of the detrital charcoal samples from the base of Qyc1 were reworked from an older deposit, but it seems unlikely that reworked samples would be more abundant than samples that are contemporaneous with the deposit. (4) Finally, OSL dates from Qyw1 (see following) partly overlap with the OSL dates for Qyc1, further supporting our contention that the OSL dates from Qyc1 are anomalously young (most likely due to bioturbation) and do not accurately represent the depositional age of that deposit. Thus, we use the radiocarbon results to infer that the terrace tread that forms the top of Qow3b was abandoned at ca. 34.9 ka, as Plunge Creek began an incision cycle that would lead to the Qow3b/Qyw1 riser and to its likely counterpart, an offset channel wall on the southeast side of the Qvof knob (described in the upcoming section "Offset channel wall").

Qyw1: Latest Pleistocene to early Holocene fluvial deposits. A younger strath terrace is incised even deeper into the Qow3a fill than the Qow3b cut terrace. The tread of this terrace is ~25 m above the modern channel, and it is underlain by 8–10 m of Qyw1 gravel, with rounded granitic boulders, mostly ≤0.5 m in diameter, deposited on a strath surface cut into gneissic bedrock. Two OSL samples (PCSR13 and 14) from an unbioturbated sand layer within stratified Qyw1 deposits that were exposed in cut 5 (see Data Repository sheet 1[1]) have been dated at 14.1 ± 1.4 ka and 15 ± 1.2 ka (Table 2).

The riser that formed when Plunge Creek incised from the Qow3b cut terrace down to the Qyw1 strath terrace forms the basis for our estimate of the slip rate for the past ~35 k.y. (see the

TABLE 3. MORPHOLOGIC DESCRIPTIONS OF SOIL PEDON FROM TRENCH 1 ON Qyc1 AT THE PLUNGE CREEK SITE

Horizon	Depth (cm)	Boundary	Dry color	Moist color	Texture	Gravel (%)	Structure	Consistence	Clay linings	Comments
B1	54–67	aw	10YR4/3	10YR3/3	SL	≤5	2msbk	SH; SS, PS	v1vn	
B2	67–84	cw	7.5YR3/2 & 4/4	7.5YR3/2	L-CL	≤5	3msbk	H; S, PS	v1k, 2mkpf	Mottled colors from clay films
B3	84–136	gw	7.5YR4/6 & 3/2	7.5YR3/4	SCL	≤5	3 co&msbk	VH; S, P	2mk, 1kpf	
B/C	136–172		7.5YR6/4-6/6 overall 7.5YR4/2 cf	7.5YR4/4	SL+	<5	2msbk	VH; SS, SP	v1mk, 1n pf	Tongues of Bt extend into this horizon and comprise 50%–60% of the total.
B/C2	172–212	cw	7.5YR5/4	7.5YR5/4	SL	≤5	2+msbk	VH; SS, VPS	v1nbr	
B/C3	212–314		10YR5/4	10YR4/4	SL	≤5	1m&cosbk-abk	H; VSS, SP	v1n pf	Clay films along "sheets" or fracture faces (~50 cm apart) and some in bands.

Note: abbreviations used here are defined in Schoeneberger et al. (1998) and in Appendix 1 of Birkeland (1999).

[1]GSA Data Repository item 2012288, which provides annotated logs of trenches and construction cuts examined as part of this study as well as relevant logs from previous studies conducted by consultants, is available at http://www.geosociety.org/pubs/ft2012.htm or by request to editing@geosociety.org.

Downloaded from gsabulletin.gsapubs.org on January 7, 2013

upcoming section "Slip rate since ca. 35 ka"). This riser is referred to as the Qow3b/Qyw1 riser in the remainder of the paper and in Figures 4, 5, 7, and 10.

Qyc2: Early Holocene colluvial wedge. The Qyw1 terrace tread is largely covered by a colluvial wedge (Qyc2) that is > 10 m thick and is composed of unstratified, unsorted silty sand (Figs. 4 and 7). Three radiocarbon dates (PCSR-T3–8, –9, and –11) from Qyc2 range from 8.2 to 9.5 ka (Table 1; Data Repository sheet 2 [see footnote 1]).

Qyf2: Early Holocene, fine-grained alluvial fan. On the west side of Plunge Creek, where the Qow3a and Qow3b deposits hug the gneissic mountain front just northeast of the San Bernardino strand (Figs. 4 and 6), a contact between the top of the Qow3b boulder gravel and the overlying sandy deposits of Qyf2 is visible (Fig. 6). This contact is mostly planar and subhorizontal except for two divots that were probably formed when local gullies (d1 and d2 in Fig. 6) incised into Qow3b. These mild incisions were later filled by sandy deposits (Qyf2) derived from those same gullies. After filling the shallow gullies incised into Qow3b, Qyf2 continued to aggrade in the area below and south of gullies d1 and d2. These relationships will be important later in the paper, when we reconstruct the sandy Qyf2 fan across the fault. The Qyf2 deposits have only been dated on the southwest side of the San Bernardino strand (see the upcoming section "Qyf2: Early Holocene alluvium from smaller drainages").

Qyw2, Qyw3, Qyw4: Younger Holocene terraces. Minor fill terrace remnants are present locally within the gorge incised into bedrock below Qyw1. These include Qyw2, Qyw3, and Qyw4, at elevations of 4–5 m, ~2 m, and ~1 m, respectively, above the modern channel. None of these units has been dated, but they are inferred to be Holocene, on the basis of their geomorphic position inset into Qyw1.

Relations Southwest of the Fault, Proposed Correlations, and Geologic History of the Surficial Units

In this section, we describe the geologic units southwest of the fault, we propose correlations of these units to the previously described units northeast of the fault, and we outline our view of the geologic history of the surficial units at this site. Our proposed geologic history is summarized in the reconstructions shown in Figure 11, which we refer to throughout this section. More detailed justification of the two correlations that we use to estimate slip rates across the San Bernardino strand is given in the "Latest Pleistocene Slip Rate for the San Bernardino Strand at Plunge Creek" section.

Qvof knob. On the southwestern side of the San Bernardino strand, there is a prominent knob that is cored by basement rock consisting of gneiss and diorite (Fig. 4) of the Wilson Creek block (Matti et al., 2003b). The knob is mantled by very old alluvial-fan deposits (Qvof) that have strong pedogenic development, including reddening (2.5YR 3/6–4/8 Munsell Soil Color Chart) and clay accumulation. Clasts within the Qvof deposit are almost exclusively (~97%) rounded granitic boulders and cobbles with equigranular textures, with the remainder being biotite gneissose rock derived from the Wilson Creek block. Where we examined Qvof in a construction cut on the west flank of the

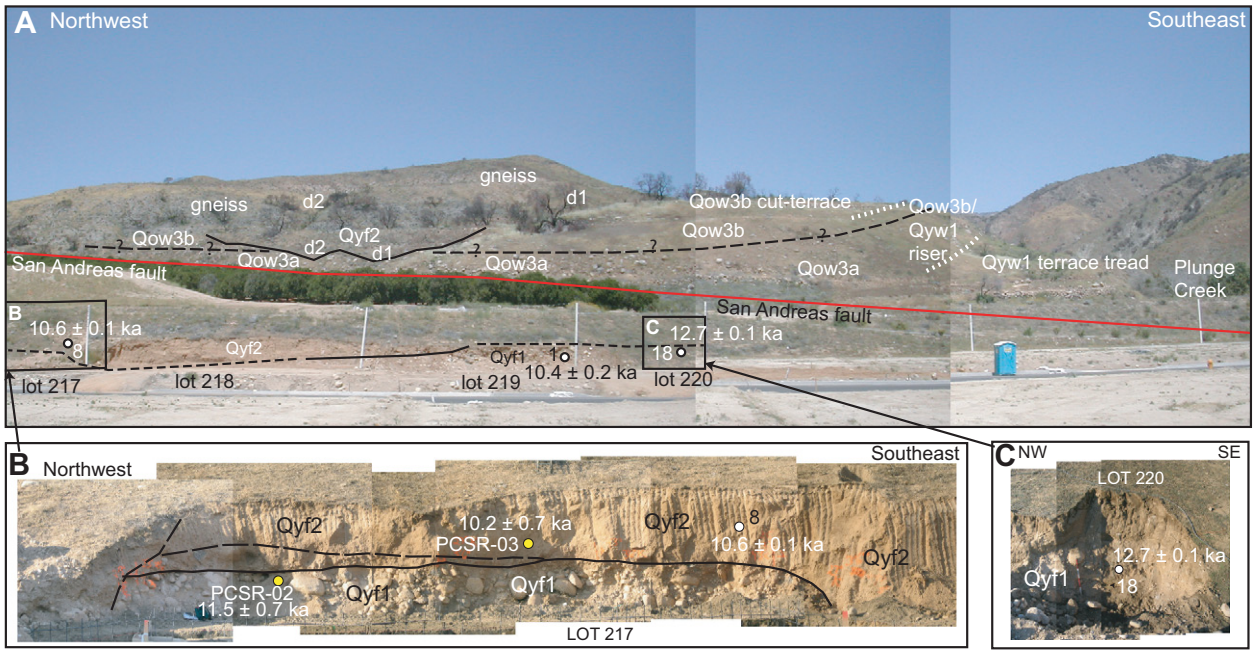

Figure 10. (A) Photomosaic looking northeast across the San Bernardino strand of the San Andreas fault into the Plunge Creek drainage basin, showing treads of the Qow3b and Qyf1 terraces and the riser between them, which we correlate with the offset channel wall that forms the steep eastern side of the Qvof knob on the southwest side of the fault (beyond left edge of the picture). We correlate the Qyf1 gravels, exposed in construction cuts in the foreground, with the Qyw1 gravels on the northeast side of the fault. Locations (white filled circles) and calibrated ages of charcoal samples from southwest of the fault are shown. Photos taken 1 May 2004; view to northeast. Width of photomosaic is about 100 m, along the paved road in the foreground. Note blue outhouse for scale. (B) Photomosaic of construction cut on lot 217 showing location of radiocarbon and optically stimulated luminescence (OSL) samples. Photographs were taken 9 October 2004, after additional excavations had been undertaken on the construction site. View to northeast. Width of photo is about 25 meters. Height of construction cut is 2–3 m. (C) View showing radiocarbon sample location from construction cut on lot 220. Photograph was taken 22 October 2004; view to northeast. Width of photo is about 6 m. Height of construction cut is about 3 m.

Downloaded from gsabulletin.gsapubs.org on January 7, 2013

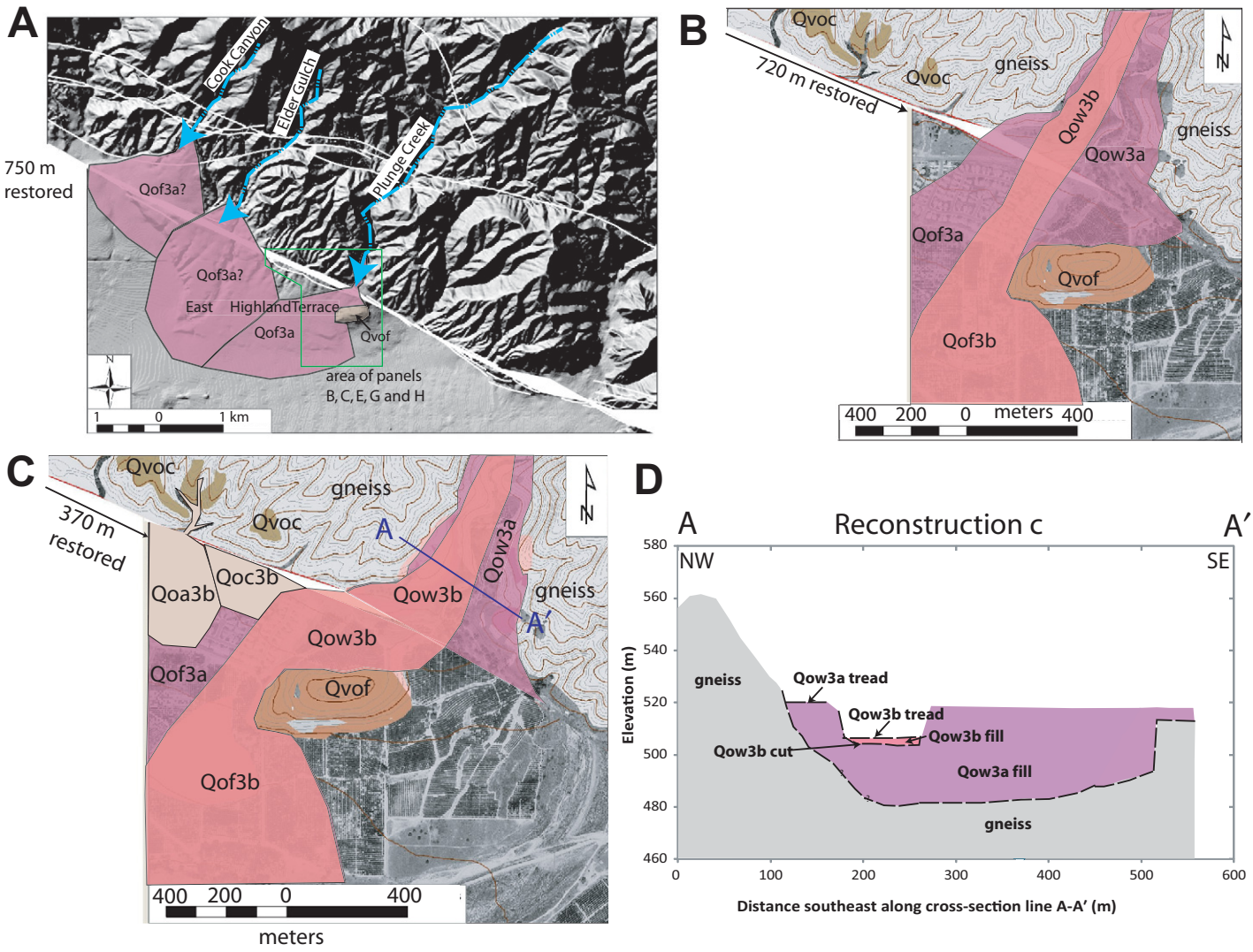

Figure 11 (*on this and following page*). Reconstructions illustrating the inferred late Quaternary geologic history of the Plunge Creek site. (A) 750 m of slip restored. Much of the East Highland Terrace is inferred to have been deposited during Qof3a time (ca. 55–70 ka) from sources in Plunge Creek, Elder Gulch, and Cook Canyon. Area of part A is the same as area of Figure 2. Green polygon outlines the area shown in frames B, C, E, G, and H. The area shown in each of these frames is the same as that shown in Figure 4. (B) 720 m of slip restored. Qow3b incises into Qow3a and Qof3a. (C) 370 m of slip restored. Qow3b has developed a kink due to offset along the San Andreas fault. (D) Cross-section A-A′, applicable to the reconstructions shown in B and C. The original width of the Qow3b cut terrace and overlying thin veneer of fill is unknown, but it is drawn here to be about the same width as the abandoned channel southwest of the fault, through which Plunge Creek is inferred to have flowed during Qof3b time.

knob, clasts are mostly <40 cm, but boulders up to ~1 m in diameter are present locally (Data Repository sheet 3 [see footnote 1]).

Matti et al. (2003b) assigned an early middle Pleistocene age to this unit. We collected and analyzed one OSL sample (PCSR-04) from a sand layer within Qvof that was exposed in construction cut L44-52 (Fig. 4; Data Repository sheet 3 [see footnote 1]). Unfortunately, the OSL signal was saturated, and an age could not be determined (Table 2).

The clast sizes and lithologies indicate the source of Qvof on this knob must have been a major drainage emanating from the San Bernardino Mountains. Given the substantial age of the deposit, it has probably been significantly offset by the fault, and the source is likely to be east of Plunge Creek. Possible sources include Oak Creek, ~1 km to the southeast, or the Santa Ana River, 4 km to the southeast. The granitic and gneissose clasts observed in Qvof are present in modern deposits of both Oak Creek and the Santa Ana River. The modern Santa Ana River deposits also contain minor amounts (~1% or less) of other lithologies (e.g., megaporphyritic monzogranite, quartzite, and mica-poor gneiss) that were not observed in Qvof at Plunge Creek. However, a systematic search for these lithologies within Qvof was not conducted at the time that large expanses of Qvof were exposed in construction cuts, so we cannot rule out the Santa Ana River as a potential source for Qvof at Plunge Creek.

Qof3a: Concealed and inferred late Pleistocene fan. As described previously, Qow3a formed a >400-m-wide fan where it crossed the San Bernardino strand (Fig. 4) and should therefore correlate with a large fan on the southwest side of the fault. Presumably, a significant

Downloaded from gsabulletin.gsapubs.org on January 7, 2013

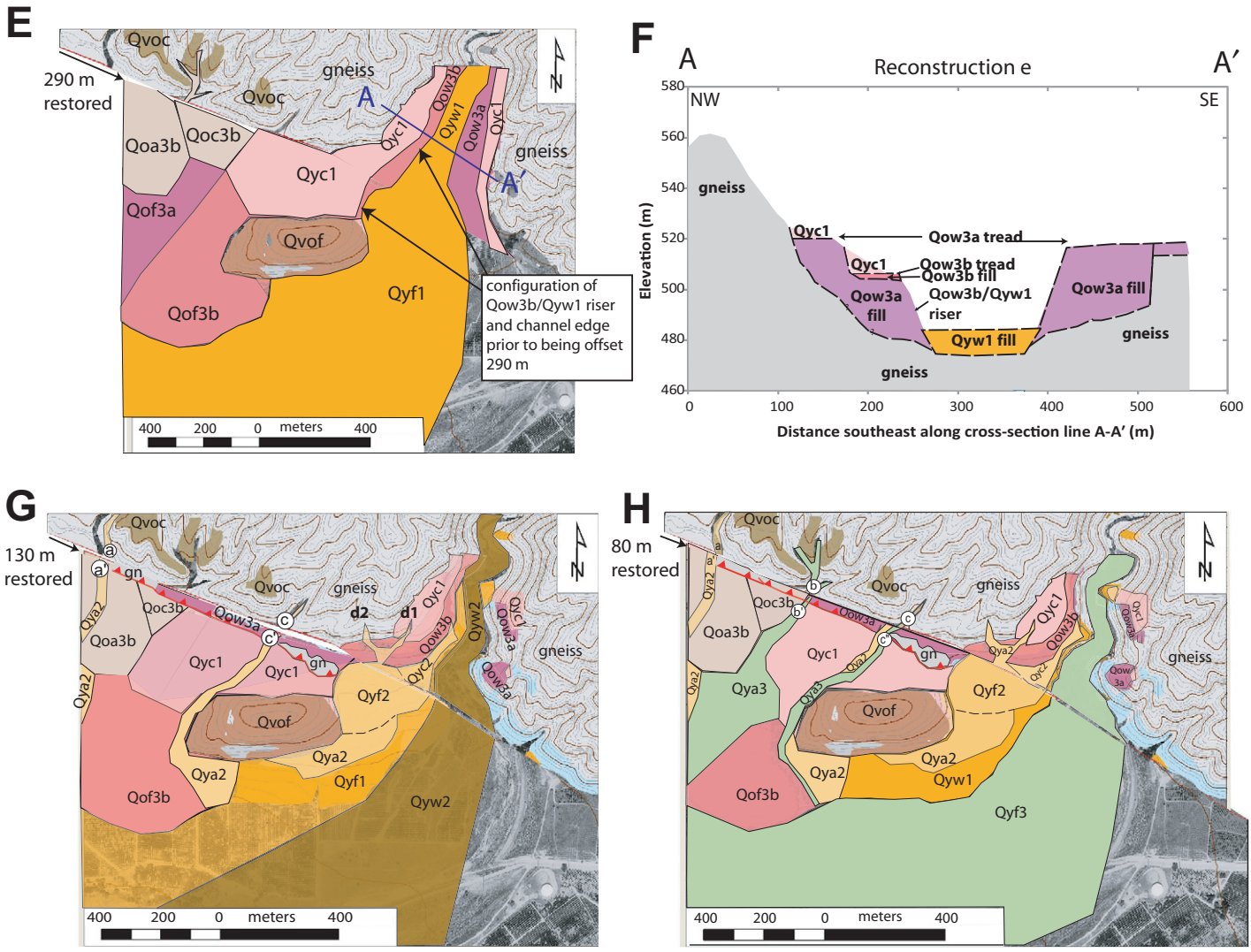

Figure 11 (*continued*). (E) 290 m slip restored, which is the amount of offset that the Qow3b/Qyw1 riser would have experienced if it incised in its present position relative to the sidewalls of the canyon northeast of the fault. See Figure 13 for an alternative reconstruction in which the riser incised farther east and then migrated to its current position via lateral erosion and channel widening. (F) Cross-section A-A′ applicable to reconstruction E. (G) 130 m of slip restored. Broad apex of the fine-grained, Qyf2 fan southwest of the fault is aligned between inferred source gullies d1 and d2. Gullies aa′ and cc′ are also in alignment. (H) 80 m of slip restored, i.e., a reasonable offset estimate of the Qyf1/Qyf3 riser, which is buried near the fault, but is loosely constrained by trench exposures of Qyf1 (see Fig. 4). Gullies bb′ and cc″ are also in alignment.

portion of the East Highland Terrace (Figs. 2 and 11A) is underlain by alluvial-fan deposits derived from Plunge Creek, including some of Qof3a age or older. Unfortunately, the East Highland Terrace is largely covered by housing developments, and exposures of the underlying deposits are limited. Exposures along the west edge of the terrace, where it is incised by City Creek, are largely pebbly sand, suggesting that one of the smaller drainages northwest of Plunge Creek was the source of the western portion of the terrace. Boulders do crop out in the walls of Bledsoe and Elder Gulches (Fig. 2), within 100 or 200 m south of the San Bernardino strand, suggesting a larger drainage, such as Elder Gulch or Plunge Creek, may be the source for the central portion of the East Highland Terrace. Between Elder Gulch (Fig. 2) and the Qof3b fan in the southwest corner of Figure 4, we have not seen what underlies the finer-grained deposits from smaller drainages that are described in the upcoming section "Qoa3b and Qoc3b: Late Pleistocene(?) fine-grained alluvium and colluviums."

The age of Qow3a is not directly known, so our reconstruction of Qow3a/Qof3a shown in Figure 11A is speculative. We speculatively show the entire East Highland Terrace deposited during Qof3a time, from Plunge Creek, Elder Gulch, and Cook Canyon. However, it is also possible that pre-Qof3a deposits from Plunge Creek underlie parts of the northwestern portion of this large terrace.

Qof3b: Late Pleistocene(?) fan and channel deposits from Plunge Creek, related to the "abandoned channel." Between the Qvof knob and the San Bernardino strand, there is a swale as wide as 100–200 m that slopes gradually to the west. We interpret this swale as an abandoned channel of Plunge Creek that was deflected by the knob and that flowed west until it reached the knob's west end, where the channel turned southwest (Figs. 11B and 11C). Southwest of the knob, topographic contours suggest the presence of a fan-shaped landform (Fig. 4). Most of

Downloaded from gsabulletin.gsapubs.org on January 7, 2013

this landform is presently covered by housing tracts, but boulder gravel is exposed at its southwestern corner. We interpret this landform as an alluvial fan deposited by the abandoned channel that flowed through the swale north of the Qvof knob. For reasons that are explained in the upcoming section "Justification of the cross-fault correlation" (for the slip rate since ca. 35 ka), we correlate this fan with Qow3b on the northeast side of the fault and thus assign this fan to unit Qof3b. We have no age control on Qof3b.

A consultant's trench was excavated in the swale in 1999 (R1–99 on Fig. 4) and was viewed briefly in the field by one of the authors (McGill). Within the southwesternmost 30 m of this trench, rounded granitic boulders, many with long axes of 0.6–1.0 m, were exposed at depths of >2.2 m, beneath artificial fill and colluvium (G. Rasmussen, 1999, written commun.; see Data Repository sheet 4 [see footnote 1]). The size, the rounded nature, and the granitic lithology of these boulders indicate that they were not derived from the gneissic bedrock of the local mountain front. They must have come from Plunge Creek or from some other large drainage that extended far enough northeast to reach granitic lithologies and was large enough to transport boulders of this size. We infer that these boulders may be deposits of Qow3b that flowed through the abandoned channel. An alternative interpretation is that these boulders are part of Qvof. The latter interpretation seems less likely because the boulders exposed in the trench are slightly larger than the average boulder size within Qvof.

Strip of Qof3a or Qof3b along and southwest of the San Bernardino strand. A strip of gravel composed of rounded granitic boulders up to 0.5 m in diameter is present along the northern margin of the swale, just southwest of the San Bernardino strand (Fig. 4). We have no quantitative age constraints on this strip of gravel. It lacks the strong pedogenic reddening that the Qvof gravel commonly displays, so it most likely is either Qof3a (alluvial-fan deposits that are correlative with the Qow3a wash deposits) or Qof3b deposits of the abandoned channel that flowed through the swale, or some combination thereof. On the basis of our reconstructions of slip across the fault (Fig. 11C), we infer that Qof3b was at one time deposited in this location. However, as discussed in the following paragraph, this strip of gravel has probably been uplifted along a reverse or oblique fault parallel to and southwest of the San Bernardino strand. It seems likely that the thin veneer of Qof3b that may once have mantled Qof3a here may have been eroded. We thus label this strip of gravel "Qof3a?" in Figure 4. Fortunately, this interpretation is not critical for our slip-rate estimate.

This strip of gravel forms a relatively steep ramp from the swale up to the San Bernardino strand, and we infer it to have been uplifted along a thrust and/or reverse fault (or oblique-slip fault) that forms part of a flower structure along the southwest side of the San Bernardino strand (Figs. 4 and 11G). Consultant's trenches (S1, S3, and S4) near the northwest corner of Figure 4 reveal a near-vertical fault along the San Bernardino strand, and a steeply to moderately north-dipping fault several meters valleyward that places gneiss over alluvium (D. Schwartzkopf, 2011, written commun.; see Data Repository sheet 5 [see footnote 1]). At the eastern end of the gravel strip, preconstruction aerial photographs show a lobate mound extending 60–100 m valleyward from the San Bernardino strand (east of the offset drainage labeled c″ in Fig. 4). A southwestward-sloping construction cut parallel to the strike of and just southwest of the San Bernardino strand passed through this lobate mound, exposing gravel in the upper part of the cut, underlain by gneiss. This cut-slope is labeled "lot W" on Figure 4 and is shown in Data Repository sheet 6 (see footnote 1). We interpret this mound as a result of uplift along the reverse- or oblique-reverse-slip fault exposed in trenches S1, S3, and S4, which may flatten to the east of channel cc″, bringing the hanging wall farther out onto the surface of the swale. The causal fault was not exposed in the construction cut at lot W. Both the gravel and the underlying gneiss within this strip are at a higher elevation than their inferred counterparts beneath the swale, consistent with uplift along a fault with a thrust or reverse component of motion located parallel to and southwest of the San Bernardino strand.

Qoa3b and Qoc3b: Late Pleistocene(?) fine-grained alluvium and colluvium. Near the northwest corner of the area shown in Figure 4, we attribute to Qoa3b and Qoc3b relatively massive, sandy deposits that are exposed in one gully and were mapped by consultants in trenches S3 and S4. Based on the size and shape of the deposit as expressed by topographic contours (Fig. 4), Qoa3b is inferred to be a fine-grained alluvial fan that emanated from a small drainage, such as the gully labeled "b" in Figure 4, and Qoc3b is interpreted to be colluvium derived from the mountain front east of gully "b." The separation of the Qoa3b apex from gully b (~370 m) is consistent with our inferred reconstruction for the time that Qow3b/Qof3b were being deposited (Fig. 11C), hence our attribution of these deposits to that same age range. We do not estimate a slip rate based on the tentative correlation of Qoa3 with gully "b," but merely present it as a reasonable interpretation that is consistent with our proposed geologic history of the area.

Offset channel wall. The Qvof knob and the swale that we interpret as an abandoned channel are truncated on the east by an erosional landform that is probably an old channel wall (Fig. 4). No other process can be reasonably inferred to have cut the steep slope at the east edge of the knob and swale. This feature was observed in the field prior to grading of the site (Fig. 3). It is also prominent in the topographic contours generated from a digital elevation model of the area with 10 m resolution (Fig. 4). Unfortunately, the higher-resolution, B4 LiDAR imagery was acquired after this site had been graded for development, but even so, the steep slope at the east edge of the knob and swale is readily apparent on this imagery (Fig. 5). As will be explained in the upcoming section "Justification of the cross-fault correlation" (for the slip rate since ca. 35 ka), we correlate this erosional feature with the Qow3b/Qyw1 terrace riser northeast of the fault.

Qyf1: Latest Pleistocene to early Holocene fan deposits from Plunge Creek. East of the Qvof knob, granitic-boulder gravel that we assign to Qyf1 was exposed in construction cuts on lots 217, 219, and 220. Two radiocarbon dates on detrital charcoal and one OSL date indicate an age of 10.4–12.8 ka for the Qyf1 gravels southwest of the fault (Fig. 10; Tables 1 and 2). These ages support a correlation of Qyf1 with Qyw1 on the opposite side of the fault. We infer that both were deposited by Plunge Creek after it incised below the level of Qow3b and the abandoned channel (Fig. 11E). This correlation is also supported by topographic profiles, and is justified in more detail in the upcoming section "Justification of the cross-fault correlation" (for the slip rate since ca. 35 ka).

Gravel deposits of similar age to Qyf1 were exposed in trenches P2 and P6 on the southeast side of Plunge Creek (Fig. 4) during two previous studies (McGill et al., 2002; S.C. Suitt, 1992, written commun.). Radiocarbon dates on detrital charcoal from pebbly gravel just northeast of the San Bernardino strand in trenches P2 and P6 (Fig. 4) are 10.4 ± 0.2 ka and 13.2 ± 0.2 ka (Table 1). These deposits are not as coarse as the Qyf1/Qyw1 gravels of Plunge Creek, nor are they as high in elevation. Their source may have been Oak Creek, which is a smaller drainage basin than Plunge Creek, or their source may have been the even smaller gully near trenches P2 and P6 of the paleoseismic site. Regardless of their origin, accumulation of these deposits at the same time as Qyf1/Qyw1 from Plunge Creek is consistent with a period of latest Pleistocene–early Holocene aggradation. The Qyf1 gravels in trenches P2 and P6 are underlain by colluvium. Two radiocarbon dates

Downloaded from gsabulletin.gsapubs.org on January 7, 2013

from this colluvium in trench P1 are 22.4 ± 0.4 and 25.9 ± 0.8 ka, suggesting that accumulation of Qyf1 began sometime after this.

Dates from Cajon Creek, ~30 km northwest of Plunge Creek, also indicate a period of aggradation at the same time as the Qyw1 and Qyf1 were accumulating in Plunge Creek (Weldon, 1986; his Qoa-c unit).

Qyc1: Late Pleistocene(?) colluvium. As mentioned previously, the consultant's trench R1–99 exposed granitic boulder gravel (which we interpret as Qow3b) beneath >2.2 m of brown, silty sand (G. Rasmussen, 1999, written commun.; see Data Repository sheet 4 [see footnote 1]). We interpret the silty sand as colluvium (Qyc1) shed from the mountain front into the abandoned channel after it was abandoned by incision of Plunge Creek down to the Qyw1/Qyf1 level (Fig. 11E).

Qyf2: Early Holocene alluvium from smaller drainages. Immediately southwest of the San Bernardino strand, Qyf1 is buried by a sandy alluvial fan (Qyf2) that has a broad apex at the fault, east of the Qvof knob. Construction cuts exposed the distal portion of this fan, where it consists of 1–2 m of silty sand overlying Qyf1 boulder gravel (Fig. 10; see L217, L219, L220 in Fig. 4 for location). The source of this small fan is inferred to be gullies d1 and d2, now right-laterally separated from the fan apex by 130 ± 70 m (Figs. 4, 6, and 11G). This correlation is further justified in the upcoming section "Justification of the cross-fault correlation" (slip rate for the past ~10.5 k.y.), where we use the offset of this fan to estimate the Holocene slip rate of the San Bernardino strand. One OSL date and one radiocarbon date on detrital charcoal are in agreement that the base of the distal portion of the Qyf2 fan is 10.2–10.6 ka. This is comparable in age to the Qyc2 colluvium that buries Qyw1 northeast of the fault.

Three other small drainages, a-a′ and c-c′ in Figure 4 and Bledsoe gulch in Figure 2, are offset by an amount within the range reported for Qyf2 (Table 4; Fig. 4). Drainage a-a′ (offset 140 ± 10 m), drainage c-c′ (offset 145 ± 25 m), and Bledsoe Gulch (offset 125 ± 10 m) may have incised within the same general time period as incision of gullies d1 and d2 (Fig. 11G), suggesting that the Pleistocene-Holocene boundary may have been a climatic period in which small drainages were incising the mountain front, if our correlations are correct. In Figure 4, we attribute the deposits within drainages a-a′ and c-c′ to Qya2.

TABLE 4. OFFSET DRAINAGES NEAR PLUNGE CREEK

Name	Label on figure	Offset (m)*
Bledsoe Gulch	BG in Fig. 2	125 ± 10
Elder Gulch	EG in Fig. 2	50 ± 10
Unnamed	a-a′ in Fig. 4	140 ± 10
Unnamed	b-b′ in Fig. 4	80 ± 15
Unnamed	c-c′ in Fig. 4	145 ± 25
Unnamed	c-c″ in Fig. 4	95 ± 10

*Offsets were measured using the B4 light detection and ranging (LiDAR) imagery, in conjunction with a digital orthophotoquad from the mid–twentieth century, except for c-c′, which was measured from the (older) 10 m digital elevation model because channel c″ had been filled with artificial fill by the time the B4 LiDAR imagery was acquired.

Qyf3: Holocene alluvial-fan deposits from Plunge Creek. A large terrace is underlain by deposits of Qyf3, inset into Qyf1 on the southwest side of the San Bernardino strand (Fig. 4). The terrace riser separating Qyf1 from Qyf3 is visible on stereo aerial photographs and is locally preserved within orange groves today, but much of this area had been developed or was in the process of being developed at the time the mapping was done for this study. Unfortunately, even on predevelopment aerial photographs, the portion of this riser within 200 m southwest of the fault is buried beneath Qyf2, so its precise intersection with the fault is difficult to infer. Exposures of Qyf1 in lots 217, 219, and 220 (Fig. 4) indicate that the riser must be east of these exposures. A dotted, queried contact in Figure 4 shows the westernmost possible position of this riser beneath Qyf2. This yields a maximum offset of ~80 m when matched with the eastern edge of Qyw1 northeast of the San Bernardino strand. In Figure 11H, we show a reconstruction that restores 80 m of slip, aligning gully b with gully b′, and aligning a speculative but reasonable position for the initial incision of the Qyf1/Qyf3 riser. The offset of gully cc″ is only slightly larger than this (95 ± 10 m), suggesting that it may also have incised within this general time frame. We have no age constraints from Qyf3.

LATEST PLEISTOCENE SLIP RATE FOR THE SAN BERNARDINO STRAND AT PLUNGE CREEK

We estimate slip rates for the San Bernardino strand for two separate periods defined by degradational and aggradational events that we correlate across the fault:

(1) a slip rate for the period since the "offset channel wall" southwest of the San Bernardino strand was displaced away from the Qow3b/Qyw1 riser northeast of the fault over the past ~35 k.y.; and

(2) a slip rate for the period since the fine-grained Qyf2 fan southwest of the San Bernardino strand was offset from gullies d1 and d2 northeast of the fault over the past ~10.5 k.y.

The slip rate over both of these time periods is remarkably similar, that is ~7–16 mm/yr.

Slip Rate since ca. 35 ka

As described already, we infer that when Plunge Creek incised from the Qow3b level to the Qyw1 level at ca. 34.9 ka, this created two features, which we correlate across the San Bernardino strand: (1) the steep terrace riser separating units Qow3b and Qyw1 on the northeast side of the fault and (2) the steep slope on the southeast side of the Qvof knob (Fig. 5). We interpret the latter as the downstream continuation of the terrace riser between Qow3b and Qyw1; hence, in Figures 3, 4, and 5, we refer to this feature as an offset channel wall that has been displaced and is now separated by ~290 m from the Qof3b/Qyw1 terrace riser. In our slip-rate estimate based on this erosional feature, we interpret the relatively well-documented ca. 34.9 ka age of abandonment of Qow3b to represent the age of initial incision of this riser. Next, we discuss how we justify this cross-fault correlation and how we constrain the amount of offset since the time of this initial incision.

Justification of the Cross-Fault Correlation

Our proposed correlation implies that the top of the boulder gravel exposed in trench R1–99 within the abandoned channel north of the Qvof knob correlates with the terrace tread that forms the top of Qow3b northeast of the fault (Fig. 11C). The presence of the small, bouldery fan at the southwest corner of the Qvof knob suggests that Plunge Creek did indeed flow through the swale north of the Qvof knob at sometime in the past, probably beginning during Qo3a time and continuing during Qo3b time. The terrace tread that forms the top of Qow3b is of similar width (Figs. 4 and 7) and an appropriate elevation (Fig. 12) to correlate with the abandoned channel within the swale. Most importantly, the Qyw1 fluvial gravels that were deposited against the Qof3b/Qyw1 riser northeast of the fault are similar in age to the Qyf1 gravels that were deposited against the offset channel wall southwest of the fault, which supports the correlation of these two erosional features across the fault. OSL dates from Qyw1 northeast of the fault at a depth of at least 2.5 m below the surface (Data Repository Sheet 1 [see footnote 1]) are slightly older (11.3–17.4 ka; Table 2, samples PCSR 13 and 14, using 2σ uncertainties) than but overlap with the radiocarbon and OSL dates from within <1 m below the top of Qyf1 exposed southwest of the fault in construction cuts L217–L220 (10.3–12.9 ka; C-14 samples 1 and 18 in Table 1 and PSCR02 in Table 2). Dates from the colluvium immediately overlying Qyw1 and Qyf1 are also similar on both sides of the fault (8.0–9.6 ka northeast of the fault [samples T3–8, T3–9, and T3–11 in Table 1] and 9.5–10.9 ka southwest of

Downloaded from gsabulletin.gsapubs.org on January 7, 2013

the fault [sample 8 from Table 1 and PCSR03 from Table 2).

We did consider other potential correlations that would have matched the steep slope on the southeast side of the Qvof knob (1) with the riser between Qow3a and Qow3b (this riser is now buried beneath Qyc1), or (2) with the riser between Qyw1 and Qyw3 (Fig. 7). Neither of these correlations is consistent with the dated samples, and the second one also has the problem of requiring a significant amount (20–30 m) of southwest-side-up slip on the San Bernardino strand within the past ~10 k.y. (Fig. 12). To our knowledge, southwest-side-up slip has not been noted anywhere else along the San Bernardino strand. Our preferred correlation does itself require a slight amount of southwest-side-up displacement (~4 m; Fig. 12). We discount this as a negligible amount, however, given the uncertainties in cross-fault projections (see caption to Fig. 12).

Figure 12 (*on following page*). Topographic profiles along Plunge Creek and its terraces. See Figure 4 for locations of profile lines B-B′-B″ and C-C′, but note that the northeast end of profile B-B′-B″ is 740 m father upstream beyond the northeast edge of Figure 4. Filled symbols represent elevations taken from a 10 m digital elevation model (DEM) of the region (U.S. Geological Survey, national elevation data set). Wide scatter in the elevations of some terraces may represent errors in the terrace elevations estimated in the field using hand-held global positioning systems (GPS), where terrace surfaces were accessible, and using an inclinometer to sight inaccessible terrace remnants. Open symbols mark terrace elevations that were surveyed with a total station. Points at the top and base of Qow3a are in red and bright pink, respectively; blue symbols mark points at the top of Qow3b northeast of the fault and along the abandoned channel southwest of the fault. Points along the top and base of Qyw1 are in green and teal, respectively. Modern channel is marked by black symbols. Elevations of Qow3b southwest of the fault (in the abandoned channel, profile) were taken from the 10 m DEM along profile C-C′ but have had 2.7 m subtracted, representing the thickness of colluvium observed on top of the Qof3b(?) gravel in trench R1–99 (Fig. 4). Additional uncertainty in the elevation at which profile C-C′ projects to the fault stems from the unknown length of the southeasternmost portion of the abandoned channel, which was destroyed when Plunge Creek incised down to Qyw1 level (see curved, dashed blue line in Fig. 4 for the inferred length that is used in this figure).

Offset Measurement

For a piercing point on the southwestern side of the fault, we follow the offset channel wall, which is defined by the east face of the Qvof knob and the abandoned channel swale, toward the fault (Figs. 4 and 5). This is a curved feature, as channels can be. The channel wall becomes less well defined close to the fault, but it projects to the fault near the southeasternmost limit of the strip of granitic gravel (Qow3a[?]) on the southwest side of the fault. It makes sense that Qow3a(?) would be preserved to the northwest of the intersection of the channel wall with the fault and removed to the southeast of that intersection, as a result of the incision of Plunge Creek down to the Qyw1 level. This lends confidence to the projection of the curved channel wall to the fault. We use the southeastern limit of Qow3a(?) gravel on the southwest side of the fault for our preferred piercing point southwest of the fault (light-blue square with solid border in Figs. 4 and 5). However, we allow that this gravel may have extended farther southeast prior to erosion, so for a southeastern bound on the location of the piercing point southwest of the fault, we project the base of the geomorphic expression of the channel wall to the fault (curved, dashed white line in Fig. 5). We also acknowledge that the thrust fault that we infer southwest of the San Bernardino strand complicates the choice of a piercing point on the southwest side of the San Bernardino strand. Given this uncertainty, we estimate an upper bound on the offset by projecting the northernmost expression of the offset channel wall (where it is truncated by the thrust fault) directly into the San Bernardino strand (Figs. 4 and 5).

On the northeast side of the fault, the piercing point has been removed by erosion, and we must infer its location by projecting to the fault the base of the riser between Qow3b and Qyw1. Figures 11E and 11G show a reconstruction in which we assume that the riser initially incised at its current location and that the base of the preserved portion of riser extended in a straight line to the fault. These assumptions yield a piercing point on the northeast side of the fault, which, in combination with our preferred piercing point southwest of the fault, yields an offset of 290 m of right-lateral slip (Fig. 5). If the riser trended more westerly as it approached the fault, the offset could be smaller, but using the detailed topography shown in the B4 LiDAR imagery to define the degraded portion of the riser as it approaches the fault, it seems unlikely that the riser is offset <210 m (Fig. 5).

For a maximum estimate of the offset, we acknowledge that the Qow3b/Qyw1 riser may have initially incised east of its present location, and that it may then have migrated to its current position within the drainage by lateral erosion leading to channel-widening northeast of the San Bernardino strand (while still flowing at the Qyw1 level). Figure 5 shows the easternmost possible location of initial incision of the Qow3b/Qyw1 riser. This position is constrained by the eastern limit of Qyw1 ~400 m upstream from the fault, and, closer to the fault, by outcrops of gneiss that exist at the elevation at which Qyw1 would be expected. If the channel had incised any farther east than this, it would have eroded the existing basement rock outcrops that are present there today. This yields an offset of 510 m from our preferred piercing point southwest of the fault, or a maximum of 580 m if the piercing point on the southwest side of the fault is hidden beneath the hanging wall of the minor thrust fault. An alternative reconstruction illustrating 510 m of slip restored at the time of initial incision of the Qow3b/Qyw1 riser is shown in Figure 13.

Slip-Rate Calculation

In order to combine the uncertainties in the offset and age to obtain a 95% confidence interval for the slip rate, we assign probability density functions to the offset and age that represent our judgment of the uncertainties in these measurements. For the offset, we use a trapezoidal probability density function indicating an equal likelihood of offsets between 290 m and 510 m (Figs. 5 and 14A), and with tails tapering to zero probability below 210 m and above 580 m. For the age, we construct a probability density function with a peak at the mean of the combined date distribution for C-14 samples T1–2, T1–3, and T2–8 (34.9 ka), and with tails that decrease linearly to zero at the outer ends of the 2σ error bounds for the three individual dates (32.17–36.46 ka; Fig. 14B). This yields a probability density function (pdf) for the slip rate that has a flat top from 8.3 to 14.5 mm/yr. The slip rate is most likely to be in this range, and it is equally likely to be anywhere within this range. The 95% confidence interval for the slip rate is 7.0–15.7 mm/yr (Fig. 14C).

Slip Rate for the Past ~10.5 k.y.

We also calculate a slip rate based on the age and offset of the sandy Qyf2 fan that was deposited on top of Qyf1 southwest of the fault, as described in a preceding section "Qyf2: Early Holocene alluvium from smaller drainages."

Downloaded from gsabulletin.gsapubs.org on January 7, 2013

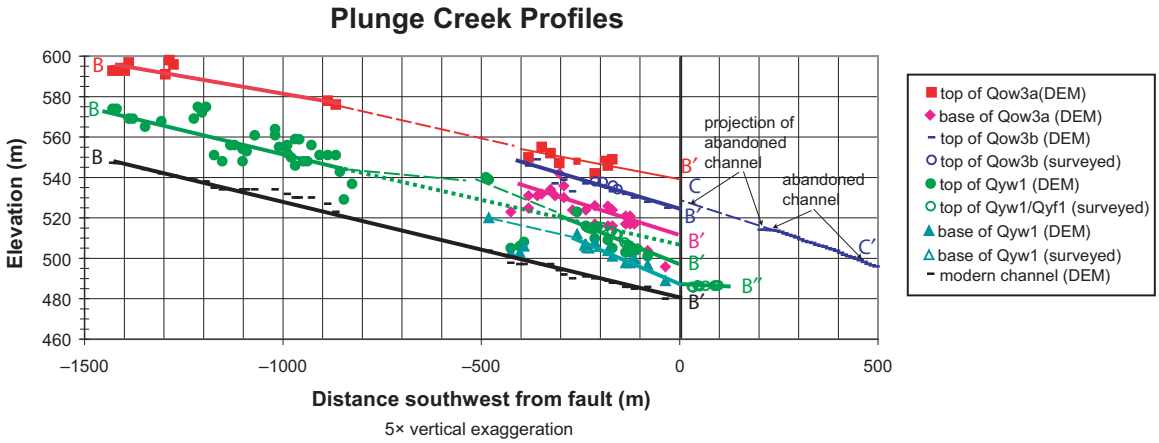

Figure 12.

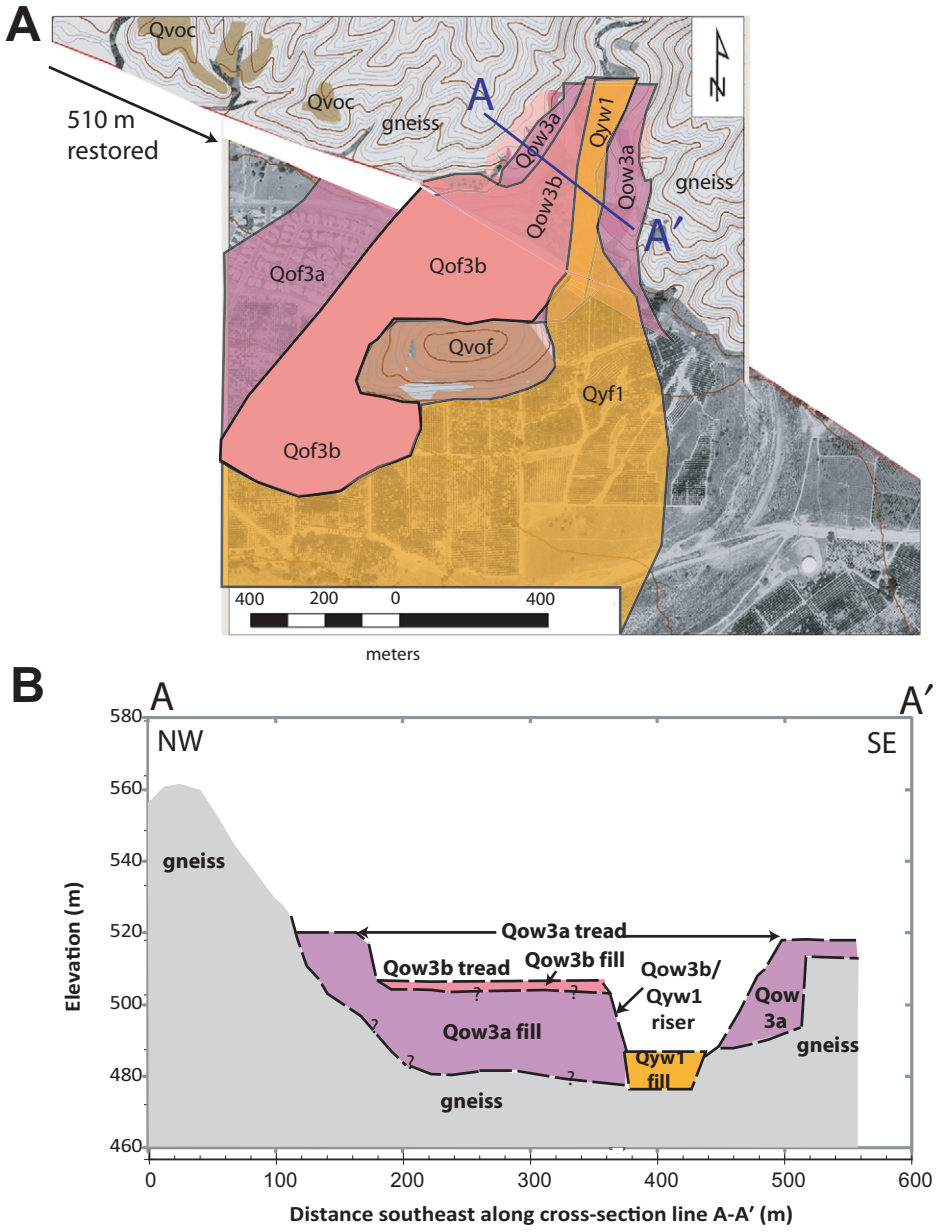

Figure 13. (A) Alternative reconstruction showing initial incision of the Qow3b/Qyw1 riser near the eastern margin of the Plunge Creek canyon, yielding a maximum 510 m offset of the riser (from our preferred piercing point southwest of the fault). (B) Cross-section A-A′ applicable to reconstruction A. In this alternate geologic history, reconstruction A would replace the reconstruction shown in Figure 11E, and cross-section B would replace the cross section shown in Figure 11F. Other aspects of the reconstructions shown in Figure 11 would remain the same.

Downloaded from gsabulletin.gsapubs.org on January 7, 2013

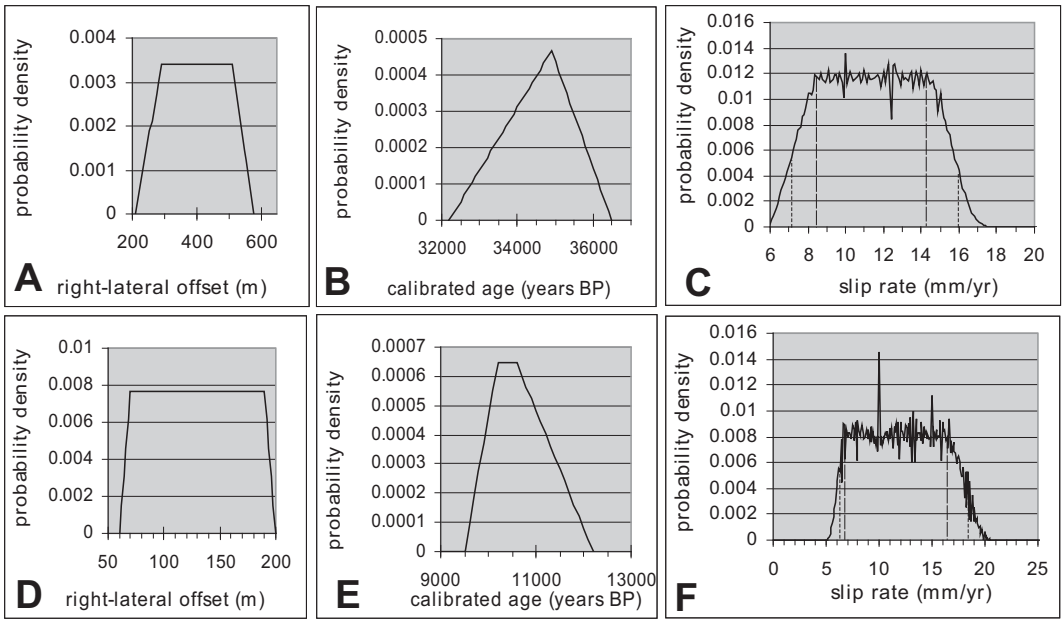

Figure 14. Inferred probability density functions (pdfs) for offset (A, D) and age (B, E) and the corresponding probability density functions for slip rate (C, F) that result from these. Upper row of pdfs (A–C) is for the slip rate for the past 35 k.y., based on offset of the Qow3b/Qyw1 riser from the channel wall that forms the southeastern margin of the Qvof knob (Fig. 5). Lower row of pdfs is for the slip rate for the past 10.5 k.y., based on the offset of the Qyf2 fan from source gullies d1 and d2 (Fig. 6). In C and F, vertical lines show the boundaries of the plateau of equal probability (long-dashed lines) and the 95% confidence interval (short-dashed lines).

Justification of the Cross-Fault Correlation

The fine-grained (sandy) nature of the Qyf2 deposits east of the Qvof knob suggests that they emanated from a small drainage along the mountain front northwest of Plunge Creek and southeast of the apex of the Qyf2 fan. Gullies d1 and d2 are the largest possible source candidates (Fig. 6).

Offset Measurement

The Qyf2 fan has a broad apex southwest of the San Bernardino strand and southeast of the Qvof knob. The center of the fan apex is marked by a yellow square in Figures 4 and 6.

Near the fault, on the northeast side, the geomorphic expression of gullies d1 and d2 is obscured beneath sandy deposits that we interpret as Qyf2 that backfilled the gullies after most of the Qyf2 fan southwest of the fault had been deposited. The surface of Qyf2 northeast of the San Bernardino strand is nearly flat and may have been modified by human activity during construction of an irrigation flume that predates 1938 aerial photographs (Figs. 5 and 6). Beneath the Qyf2 deposits, granitic boulders crop out in the slope just northeast of the San Bernardino strand. We interpret these boulders to include Qow3a with a thin veneer of Qow3b near the top. The base of the Qyf2 deposits on the slope north of the San Bernardino strand defines two swales in the top of Qow3a and/or Qow3b that were probably cut by gullies d1 and d2. We use the projections of these two swales to the fault to define the northwestern and southeastern limits of the piercing point on the northeast side of the fault, and we use the midpoint between these two points as our preferred piercing point to match with the apex of the Qyf2 fan southwest of the fault. This yields an offset of 130 ± 70 m (Figs. 6 and 11G). Restoration of the Qyf2 apex requires little or no vertical slip.

Most of the uncertainty in this offset is due to the broad width (~120 m) of the apex of this fan, and we are not certain which part of this apex was aligned with the source gullies at the time that our dated samples were deposited near the toe of the fan. We thus think it equally likely that the offset ranges between 70 and 190 m, and we represent this using a trapezoidal probability density function with a plateau from 70 to 190 m, with the remainder of the uncertainty distributed into the tails of the trapezoid, which taper to zero at 60 m and 200 m (Fig. 14D).

Slip-Rate Calculation

The radiocarbon and OSL dates from Qyf2 in lot 217 (Figs. 4 and 10; Tables 1 and 2) indicate that the Qyf2 fan had prograded to bury Qyf1 at this location by ca. 10.2–10.6 ka. This range spans the best estimates of the ages of OSL sample PSCR03 and C-14 sample 8 from Qyf2. The agreement of these two ages suggests that sample 8 is not significantly older than the Qyf2 deposit, as can sometimes be the case with detrital charcoal. The Qyf2 deposits are massive and may have experienced some bioturbation, but C-14 sample 1 from the underlying Qyf1 gravels is unlikely to have been bioturbated. We thus think it is unlikely that the Qyf2 deposits at this location are any older than 10.6 ka (the older end of the 2σ age range for C-14 sample 1). Nonetheless, we allow for the possibility of a greater uncertainty in the age by constructing a trapezoidal probability density function (Fig. 14E) that has a flat top between 10.2 and 10.6 ka and that tapers to zero at 9.5 ka (younger end of the 1σ age range of OSL sample PCSR03 from Qyf2 itself) and at 12.2 ka (older end of the 1σ age range of OSL sample PCSR02 from a portion of the underlying Qyf2 deposits that is stratified and well sorted and thus was clearly not bioturbated).

Combining the probability density functions for the offset and the age yields a probability density function for the slip rate with a broad peak of equal likelihood from 6.8 to 16.3 mm/yr and with a 95% confidence interval of 6.3–18.5 mm/yr (Fig. 14F). One may question whether the age of the Qyf2 fan at lot 217 accurately represents the age of the fan at the apex where the offset was measured. We acknowledge that the fan may have begun forming prior to this date and may have taken some time to prograde out to the location of lot 217 and/or that deposition may have continued near the apex of the fan after it had ceased at lot 217. The broad nature of the apex of the fan may indeed indicate that it was deposited over a period of time. We suspect that some portion of the broad apex of this fan was aligned with the source gullies at the time that Qyf2 was being deposited at lot 217.

DISCUSSION

Slip Rate Decreases Southeastward

Results from our investigation at Plunge Creek indicate a slip rate for the San Bernardino strand of the San Andreas fault of ~7–16 mm/yr, both

Downloaded from gsabulletin.gsapubs.org on January 7, 2013

for the past 35 k.y. and for the past 10.5 k.y. Figure 15A presents the slip rate at Plunge Creek in comparison with other late Quaternary slip-rate estimates for the San Bernardino strand. Northwest of Plunge Creek, the slip rate decreases dramatically between Cajon Creek and Badger Canyon, probably as a result of transfer of slip to the San Jacinto fault in this region (Fig. 1). Southeast of Badger Canyon, the slip rate stabilizes, with the rate at Plunge Creek being nearly identical to that at Badger Canyon. The slip transfer to the San Jacinto fault is thus accommodated northwest of Badger Canyon, within the 16-km-long zone in which the two faults parallel each other and are only 2.5 km apart (Fig. 1). Quaternary structures within this region that may help to accommodate this slip transfer include the Peters fault and the Tokay Hill fault (Morton and Matti, 2001; Weldon, 1986). Slip transfer from the Mojave section of the San Andreas fault to the San Jacinto fault has been inferred by previous investigators (Weldon and Sieh, 1985; Matti et al., 1985, 1992; Morton and Matti, 1993; Matti and Morton, 1993). Our study helps to constrain the region within which the transfer must occur (northwest of Badger Canyon) and the amount of slip that transfers (see following).

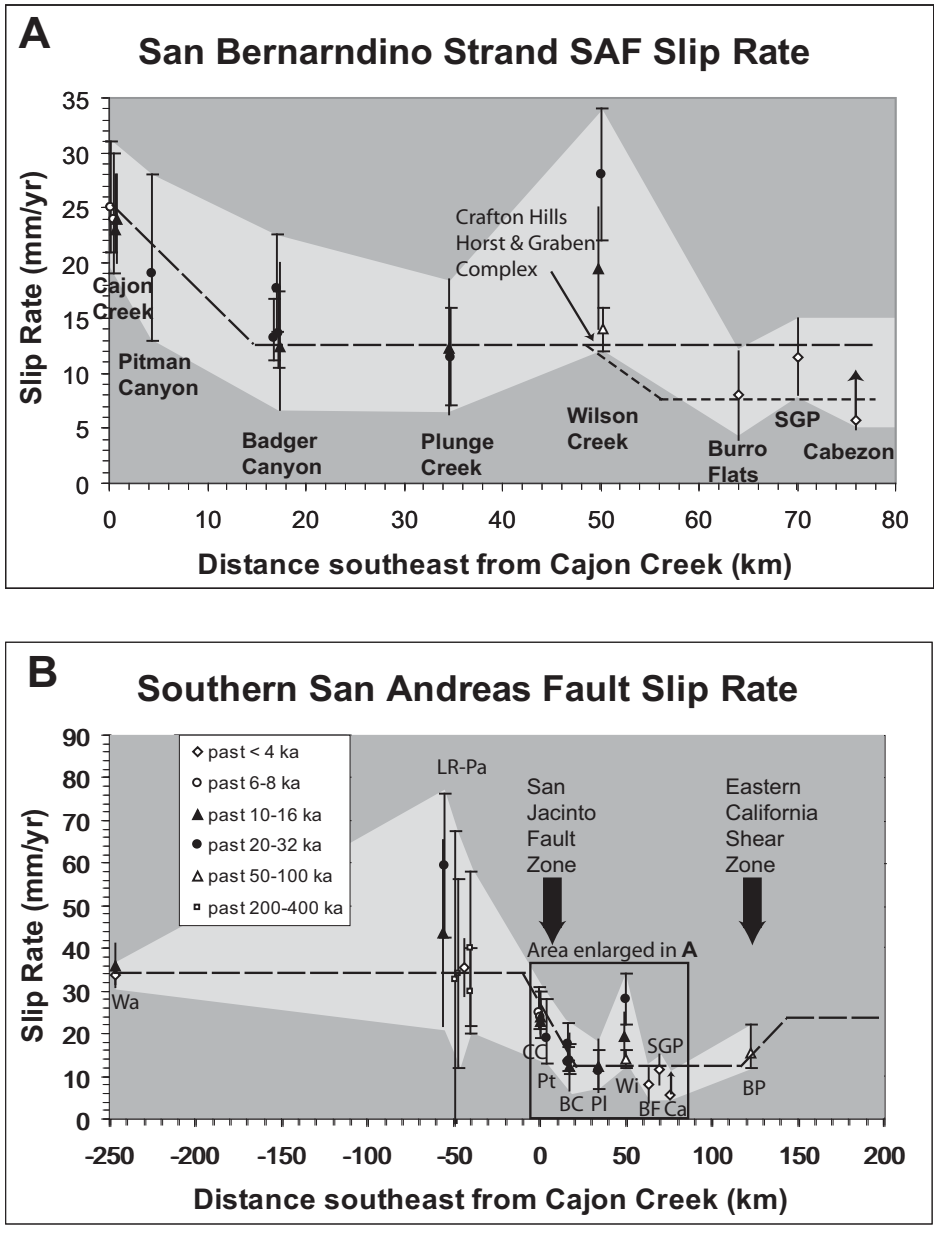

Figure 15. (A) Slip rate for the San Bernardino strand of the San Andreas fault between Cajon Creek and San Gorgonio Pass (SGP), showing southeastward decrease between Cajon Creek and Badger Canyon as a result of slip transfer to the San Jacinto fault. See part B for legend. Light-gray shading connects the minimum and maximum rates reported at each site. Dashed lines show the interpretive models proposed here. Long-dashed line shows our primary interpretation in which the slip rate decreases southeastward from between somewhere northwest of Cajon Creek and Badger Canyon as a result of slip transfer to the San Jacinto fault. In this model, lower rates at Burro Flats and Cabezon are explained by slip on other strands of the San Andreas fault zone within San Gorgonio Pass, for which rates have not been directly measured. Lower, short-dashed line shows interpretation in which additional slip transfers to the San Jacinto fault between Plunge Creek and Burro Flats via the Crafton Hills horst-and-graben complex (Fig. 1). All rates are averaged over the interval from the formation of the offset feature to the present. The Cabezon site is on the San Gorgonio Pass thrust fault, not the San Bernardino strand. The SGP value is a summary rate for the San Gorgonio Pass region, including inferred slip on other faults within the region (Yule, 2009). The published rates for Wilson Creek (Harden and Matti, 1989) are currently undergoing re-evaluation by the authors, so we do not adjust our model in an attempt to fit the anomalously high latest Pleistocene rates at that site. Other rates shown are from the following sources: Cajon Creek (Weldon and Sieh, 1985); Pitman Canyon (McGill et al., 2010); Badger Canyon (McGill et al., 2010); Plunge Creek (this paper); Wilson Creek (Harden and Matti, 1989); Burro Flats (Orozco, 2004; Yule and Spotila, 2010); Cabezon (Yule et al., 2001). (B) Slip rate of the San Andreas fault zone as a function of distance along strike from central California to the Coachella Valley. We infer that the San Andreas fault slip rate increases southeastward in the vicinity of Biskra Palms Oasis (BP), as a result of slip that is transferred from the Eastern California shear zone onto the southern San Andreas fault. Wa—Wallace Creek (Sieh and Jahns, 1984); LR-Pa—Little Rock and Pallett Creek (Matmon et al., 2005; Weldon et al., 2008; Salyards et al., 1992); CC—Cajon Creek; Pt—Pitman Canyon; BC—Badger Canyon; Pl—Plunge Creek; Wi—Wilson Creek; BF—Burro Flats, SGP—San Gorgonio Pass; Ca—Cabezon; BP—Biskra Palms Oasis (Behr et al., 2010; Fletcher et al., 2010).

Downloaded from gsabulletin.gsapubs.org on January 7, 2013

Southeast of Plunge Creek, a late Pleistocene slip rate in the low teens for the San Bernardino strand probably extends at least as far as Wilson Creek (Fig. 1), but the rate may decrease further in San Gorgonio Pass, where slip becomes distributed within a complex zone of faulting. At Wilson Creek, in Yucaipa, the slip rate of the San Bernardino strand has been 12–16 mm/yr for the past 65 or 90 k.y. (Harden and Matti, 1989), consistent with our rates at Plunge Creek. Harden and Matti (1989) reported faster rates for the past 30 k.y. and for the past 14 k.y. (Fig. 15A), but these rates are currently being reevaluated in light of new dating technologies (K. Kendrick, 2011, personal commun.).

The late Holocene slip rate on the San Bernardino strand at Burro Flats, in the San Gorgonio Pass region, is 8 ± 4 mm/yr (Orozco, 2004; Yule and Spotila, 2010), which is slightly lower than the rate at Plunge Creek (Fig. 15A). This could be a result of slip transfer to the San Jacinto Fault via the Crafton Hills horst-and-graben complex (Matti and Morton, 1993; Morton and Matti, 1993), but there are also many other fault strands within the San Andreas fault zone in San Gorgonio Pass that could be accommodating the reduced rate at Burro Flats (Yule and Sieh, 2003). Yule (2009) estimated that when other faults of the San Andreas fault zone are included, the total slip rate across the San Andreas fault zone in San Gorgonio Pass is likely 8–15 mm/yr, which is consistent with the results reported here for Plunge Creek.

Short-Term Bypass of the San Bernardino Strand

Elastic block modeling of geodetic data suggests that the San Bernardino and San Gorgonio Pass sections of the San Andreas fault are largely bypassed by plate-boundary slip. Previously published block models imply that slip on these sections of the San Andreas fault is ≤5 mm/yr, thus making up 10% or less of the total plate-boundary slip (Meade and Hager, 2005; Becker et al., 2005). Some more recent block models yield rates of 5–8 mm/yr (Spinler et al., 2010) or 8.2–10.5 mm/yr (Loveless and Meade, 2011), but these rates are still much less than the rates of strain accumulation on the portions of the fault to the northwest and southeast. In these models, a substantial portion of the slip measured on the San Andreas fault in central California is accommodated by the San Jacinto fault to the south of the Transverse Ranges, and much of the slip on the southernmost San Andreas fault transfers northward into the Eastern California shear zone (e.g., Meade and Hager, 2005; Spinler et al., 2010; Loveless and Meade, 2011).

Our results indicate that this partial bypassing of the San Bernardino section of the fault is not limited to very short geodetic time scales but has also been occurring throughout the latest Pleistocene and Holocene. We document a lower slip rate (~7–16 mm/yr) for the San Bernardino section of the San Andreas fault than for the Mojave and Carrizo sections to the northwest or the Coachella Valley section to the southeast. Within the Carrizo section, the Holocene and latest Pleistocene slip rates of the fault are 33.9 ± 2.9 mm/yr and 35.8 +5.4/–4.1 mm/yr, respectively (Sieh and Jahns, 1984) and the late Holocene rate at Van Matre Ranch is very similar (Noriega et al., 2006). Late Quaternary slip rate estimates for the Mojave section of the fault are almost all within 36 ± 8 mm/yr (Humphreys and Weldon, 1994) for a number of different time scales ranging from the past several earthquake cycles (Salyards et al., 1992; Weldon et al., 2008), to the past few thousand years (Weldon et al., 2008; Schwartz and Weldon, 1986), to hundreds of thousands of years (Weldon, 1986; Weldon et al., 1993; Matmon et al., 2005). These rates are ~3 times the slip rate on the San Bernardino section. The late Quaternary slip rate of the San Andreas fault at Biskra Palms Oasis in the Coachella Valley is 14–17 mm/yr (Behr et al., 2010). This is comparable to the rate on the San Bernardino section, but additional slip may be occurring on secondary structures northeast of the San Andreas fault in the vicinity of Biskra Palms and may join the San Andreas southeast of Biskra Palms (Fig. 1). Figure 15B summarizes Quaternary geologic slip-rate estimates for the southern half of the San Andreas fault and shows a pattern that mimics the block models of geodetic data, with a southeastward drop in slip rate where the San Jacinto fault diverges from the San Andreas and a (partly inferred) southeastward increase in slip rate where secondary faults transfer slip from the Eastern California shear zone southward onto the San Andreas fault at and southeast of Biskra Palms.

Comparison of Latest Pleistocene and Early Holocene Rates to Geodetic Rates and Implications for Hazard

It is worth noting that while the Holocene and latest Pleistocene slip rates mimic the elastic block models in general terms, confirming a partial bypassing of the San Bernardino and San Gorgonio Pass sections of the San Andreas fault at time scales averaged over hundreds to thousands of earthquake cycles, they do not mimic the block models in all respects. In particular, our latest Pleistocene and Holocene rates for the San Bernardino strand are slightly higher than some rates inferred for this fault from block models (~5 mm/yr—Meade and Hager, 2005; ~0 mm/yr—Becker et al., 2005; 5–8 mm/yr—Spinler et al., 2010). In other areas, such as the Eastern California shear zone, the rates of present-day strain accumulation (13–18 mm/yr; Spinler et al., 2010) significantly exceed rates averaged over tens or hundreds of thousands of years (<6.2 mm/yr; Oskin et al., 2008).

One possible interpretation is that the lower rates of present-day strain accumulation on the San Bernardino strand may represent fluctuations in activity between different faults within the plate-boundary system (e.g., San Jacinto, San Andreas, Eastern California shear zone) over time scales of a several earthquake cycles (e.g., Dolan et al., 2007; Weldon et al., 2004; Sharp, 1981). If that is the case, then the present-day strain accumulation rates may be more relevant than latest Pleistocene or early Holocene rates for estimating the hazards due to the next few large earthquakes in the system.

However, another possible interpretation is that differences between rates of elastic strain accumulation and rates of strain release averaged over many earthquake cycles may be the result of viscoelastic effects. The San Bernardino strand is presently at a late stage within its earthquake cycle, so viscoelastic effects could cause the present-day rate of strain accumulation to be slower than the long-term average (Savage and Prescott, 1978). The most recent large earthquake on the San Bernardino section of the fault is inferred to be the 8 December 1812 event, 200 yr ago, which is consistent with paleoseismic results from Pitman Canyon and Burro Flats (Seitz and Weldon, 1994; Seitz et al., 1997; Yule et al., 2001). Paleoseismic results from Plunge Creek suggest an even longer time (≥300 yr) since the most recent event (McGill et al., 2002). The average recurrence interval is estimated to be ~150 yr at Pitman Canyon (Fig. 1) (Seitz and Weldon, 1994; Seitz et al., 1997) and 240–310 yr at Burro Flats (Yule et al., 2001). If the present low rate of strain accumulation is indeed an artifact of the fault being late in its earthquake cycle, then the ~7–16 mm/yr rate reported here, averaged over many earthquake cycles yet over a short enough time scale to avoid major changes in tectonic regime, would be more appropriate to use in seismic hazard analysis than the slower rate of present-day strain accumulation that is implied by some elastic models.

It is also worth noting that our latest Pleistocene slip rate is consistent with one recent elastic block model (8–10 mm/yr; Loveless and Meade, 2011). Joint inversions of geologic and geodetic data (McCaffrey, 2005) also result in a slip rate (14.3 mm/yr) comparable to what we document here.

Downloaded from gsabulletin.gsapubs.org on January 7, 2013

Thus, we find no compelling reason to infer dramatic shifts in the slip rate of the San Bernardino section of the San Andreas fault over time scales of multiple earthquake cycles. The two rates we obtain at Plunge Creek indicate relative constancy of the slip rate when averaged over two different time periods: the past 10.5 k.y. and the past 35 k.y., and it is possible to interpret the geodetic site velocities in a manner that is consistent with this rate (7–16 mm/yr), either by allowing for viscoelastic effects (as described previously), or by changing the geometry of the elastic block model (Loveless and Meade, 2011), or because the uncertainties in the geodetic and geologic data are large enough to allow both data sets to be fit with a common slip rate (14.3 mm/yr; McCaffrey, 2005). We thus conclude that our 7–16 mm/yr rate is more appropriate for use in seismic hazard analysis than the 0–5 mm/yr rates obtained from some elastic block models of geodetic data (Meade and Hager, 2005; Becker et al., 2005).

Comparison of Latest Pleistocene and Early Holocene Rates to Lifetime Slip Rate

Although the slip rate on the San Bernardino strand of the San Andreas fault appears to have been stable at time scales of a few tens of thousands of years, it clearly has changed over longer time scales. Several reconstructions of bedrock across the San Andreas fault in Southern California suggest a total of 150–180 km of displacement across the San Andreas fault system (including the San Jacinto fault), since inception of this system ca. 5 Ma (Powell, 1993; Weldon et al., 1993). The reconstructions of Matti et al. (1985, 1992) and Matti and Morton (1993), which delineate the history of slip on various strands of the San Andreas fault within the San Bernardino Mountains, are particularly relevant for comparison to our results. A total bedrock offset of 140 km has accumulated across four fault strands along the San Bernardino section of the San Andreas fault zone, suggesting an average (though not necessarily constant) slip rate of ~28 mm/yr since inception ca. 5 Ma (Matti and Morton, 1993).

The combined slip rate for the past 35 k.y. of the two fault strands (San Bernardino and Mill Creek) that have been active during that time interval, however, is less than half this amount. The slip rate of the Mill Creek strand has been estimated as 2 mm/yr (R.J. Weldon II, 2010). Sieh et al. (1994) also estimated that, since the late Pleistocene, the Mill Creek fault has slipped at 10% of the rate of the San Bernardino strand (here documented to be 7–16 mm/yr). Taking both of these estimates into consideration, we consider the latest Pleistocene slip rate of the Mill Creek strand to be 1.5 ± 0.5 mm/yr. When added to the 7–16 mm/yr rate for the San Bernardino strand documented in this paper, the latest Pleistocene rate for the two faults combined is 8–18 mm/yr, which is much slower than the lifetime average slip rate across the San Andreas fault zone. This suggests that slip across the San Bernardino section of the San Andreas fault zone has been substantially faster in the past than it is today.

Slowing of the San Andreas fault is likely to have occurred when the San Jacinto fault initiated ca. 1.1–1.2 Ma (Janecke et al., 2010; Kirby et al., 2007; Lutz et al., 2006; Matti et al., 1985, 1992; Matti and Morton, 1993). Drawing on results from Matti et al. (1985, 1992), Matti and Morton (1993) suggested that the San Andreas fault southeast of Cajon Creek slowed dramatically and perhaps stopped for a time when the San Jacinto fault initiated. In this model, the initiation of the San Jacinto fault coincided with abandonment of the Mission Creek strand of the San Andreas fault after it was deformed by left-slip on the Pinto Mountain fault (Matti and Morton, 1993). Eventually, slip resumed on the San Andreas fault (though perhaps at a slower rate), with the formation of the Mill Creek strand of the San Andreas fault (Fig. 2).

Extrapolation of the late Pleistocene slip rate for the Mill Creek and San Bernardino strands combined can place constraints on the likely time of initiation of the Mill Creek fault and on the duration of any period of inactivity within the San Andreas fault zone. For example, if the combined slip rate on the Mill Creek and San Bernardino strands has been at the upper end of the 8–18 mm/yr range estimated here since initiation of the Mill Creek fault, then it would take only 0.6 m.y. to accumulate the 11 km of bedrock offset on these two strands combined (Matti and Morton, 1993). In that case, the Mill Creek fault may have initiated as late as 0.6 Ma, and the San Jacinto fault may have carried the majority of plate-boundary slip from ca. 1.1 Ma to 0.6 Ma. On the other hand, if the combined slip rate on the Mill Creek and San Bernardino strands has been closer to the lower end of the 8–18 mm/yr range estimated here, then it would take up to 1.4 m.y. to accumulate the 11 km of bedrock offset across these two strands, and no period of inactivity within the San Andreas fault zone would be required. Instead, the San Andreas fault zone could have slowed to ~8–10 mm/yr upon initiation of the San Jacinto and could have remained at that rate up to the present.

Matti and Morton (1993) inferred that the San Bernardino strand fault is quite young and evolved ca. 125 ka by partial reactivation of the older Mission Creek strand of the San Andreas fault zone. This age estimate was based on Weldon and Sieh's (1985) 25 mm/yr slip rate for the San Andreas fault at Cajon Creek. Given the 7–16 mm/yr rate we report here, it would take ~190–430 k.y. to accumulate the 3 km total offset across this strand.

Implications for the San Jacinto Fault

It has long been suggested that slip transfers between the San Andreas and San Jacinto faults in the Cajon Pass region, where the two faults approach each other (Weldon and Sieh, 1985; Morton and Matti, 1993; Matti and Morton, 1993). Our study shows that the San Andreas fault slip rate in latest Pleistocene and early Holocene time drops by 20–29 mm/yr between the Mojave (36 mm/yr) and San Bernardino (7–16 mm/yr) sections of the fault (Fig. 15B), suggesting that the amount of slip transferred to the San Jacinto fault may be quite large.

To estimate the amount of slip transferred from the San Andreas to the San Jacinto fault, we consider first three other faults that may consume part of the rate change between the Mojave and San Bernardino sections of the San Andreas fault. A few millimeters per year of slip may be consumed by the Cucamonga thrust fault and may not transfer to the San Jacinto fault. Morton and Matti (1987) suggested a convergence rate of 5 mm/yr for the Cucamonga fault using soil development for age control, but new, quantitative (cosmogenic) dates suggest a dip-slip rate of 1.9 mm/yr (Horner et al., 2007). Given the 35° dip of the fault zone (Morton and Matti, 1987), these dip-slip rates are equivalent to shortening rates of 4 mm/yr and 1.6 mm/yr, respectively. Alternatively, Weldon and Humphreys (1986) attributed Cucamonga fault slip to the geometry of the San Andreas–San Jacinto fault junction and inferred that nearly all of the San Jacinto fault slip transfers to the Mojave section of the San Andreas fault, with none being absorbed by the Cucamonga fault. To encompass this range of viewpoints, we allow that 2 ± 2 mm/yr of the 20–29 mm/yr rate difference between the Mojave and San Bernardino segments may be consumed by the Cucamonga fault, rather than transferring onto the San Jacinto fault.

The Mill Creek strand of the San Andreas fault also accommodates some of the rate difference between the Mojave and San Bernardino sections of the San Andreas fault. This fault makes its closest approach to the San Bernardino strand at Badger Canyon and diverges from the San Bernardino strand with increasing distance to the southeast. Slip on the Mill Creek strand probably eventually rejoins the main San Andreas zone in the northern Coachella Valley region. As described in the previous section, we

Downloaded from gsabulletin.gsapubs.org on January 7, 2013

infer a rate of 1.5 ± 0.5 mm/yr for the Mill Creek strand (Sieh et al., 1994; R. Weldon, 2010).

The North Frontal thrust fault, along the northern margin of the San Bernardino Mountains may also accommodate a small amount of slip from the Mojave section of the San Andreas fault, transferring this slip back to the southernmost San Andreas fault via the Eastern California shear zone. The slip rate on this fault is probably quite low. A Holocene shortening rate of 0.16 mm/yr across one strand was reported by Yule and Spotila (2010). A longer-term uplift rate of 0.6 mm/yr is obtained by dividing the maximum vertical offset of 1.6 km (Spotila and Sieh, 2000) by the post–2.5 Ma age of onset of uplift (May et al., 1982; Sadler and Trent, 1990). Using a 23° dip of the fault, this suggests a 1.5 mm/yr shortening rate, which we use in our calculations.

Thus, ~5 ± 3 mm/yr of the slip-rate decrease along the San Andreas fault may be accommodated by the Cucamonga, Mill Creek, and North Frontal faults. It would seem that the remaining 12–27 mm/yr of the rate difference must transfer to the northern San Jacinto fault. Our results thus imply a slip rate of >12 mm/yr for the San Jacinto fault and suggest that during the latest Pleistocene and Holocene, it has played at least as great a role, if not a larger role, in the plate-boundary fault system than the San Bernardino section of the San Andreas fault.

Most previously published slip rates for the San Jacinto fault fall within (or slightly below) the lower half of the 12–27 mm/yr range inferred here (Blisniuk et al., 2010, 2011; Rockwell et al., 1990; Prentice et al., 1986; Morton et al., 1986, recalculated using an older date given by Morton and Matti, 1993; Sharp, 1981), while a few fall within the upper half of this range (Janecke et al., 2010; Kendrick et al., 2002; Morton and Matti, 1993). The high rates reported by Janecke et al. (2010) (20.1 +6.4/–9.8 mm/yr) and by Morton and Matti (1993) are averaged over the lifetime of the San Jacinto Fault zone. These high rates may be reconciled with more moderate late Pleistocene rates of 12–15 mm/yr (Blisniuk et al., 2010, 2011; Rockwell et al., 1990; see Fig. 1) if the San Andreas fault stopped or dramatically slowed during the early history of the San Jacinto fault (as discussed earlier herein), allowing the San Jacinto fault to temporarily accommodate most (or all) of the ~35–36 mm/yr of slip that is thought to have been shared between the two faults for some portion of its early history (Matti and Morton, 1993; Bennett et al., 2004). This interpretation would suggest that the late Pleistocene slip rate of the San Bernardino strand is within the upper half of the 7–16 mm/yr range reported here.

On the other hand, if the late Pleistocene rate for the San Bernardino strand is within the lower half of the 7–16 mm/yr range, then that would favor a high late Pleistocene rate for the San Jacinto, consistent with the >20 mm/yr rate proposed by Kendrick et al. (2002) for the northern San Jacinto fault. A high slip rate for the northern San Jacinto fault (Kendrick et al., 2002) could be reconciled with more moderate rates of 12–15 mm/yr for the central San Jacinto fault (Blisniuk et al., 2010, 2011; Rockwell et al., 1990) if slip steps from the northern San Jacinto fault to the Coachella Valley section of the San Andreas fault via faults in San Gorgonio Pass, which extend westward toward the San Jacinto fault, as proposed by Morton and Matti (1993).

A full understanding of strain partitioning in this region has yet to be achieved, but the work presented here favors moderately low rates of slip on the San Bernardino strand of the San Andreas fault (7–16 mm/yr) since ca. 35 ka, thus implying relatively high rates (12–27 mm/yr) for the San Jacinto fault during that same time period, unless other mechanisms for accommodating the ~36 mm/yr slip rate of the Mojave section of the San Andreas fault can be found.

CONCLUSIONS

The latest Pleistocene slip rate of the San Bernardino strand of the San Andreas fault at Plunge Creek is most likely 7.0–15.7 mm/yr for the past 35 k.y., and 6.3–18.5 mm/yr for the past 10.5 k.y. Close agreement in the slip rates for these two intervals suggests constancy of the rate over periods of tens of thousands of years. These new estimates bring the latest Pleistocene slip rate closer to, but still somewhat higher than, that inferred from the rate of present-day strain accumulation.

The slip rates at Plunge Creek are about half as fast as the Holocene–latest Pleistocene rates measured for the San Andreas fault in Cajon Pass, and likely about a third of the rate farther northwest, suggesting that the slip rate decreases southeastward from the Mojave section, as a result of slip transfer to the San Jacinto fault. This slip transfer appears to occur within a 16 km length northwest of Badger Canyon in which the two faults parallel each other and are only 2 km apart. Slip rates for the San Bernardino section of the fault are comparable to most (and less than some) published slip rates for the northern and central San Jacinto fault, suggesting that, in this region, the San Andreas slips at a rate that is comparable to or less than the San Jacinto fault.

ACKNOWLEDGMENTS

This work was supported by multiple grants from the Southern California Earthquake Center. We thank Gary Rasmussen, Donn Schwartzkopf, and Jay Martin for helpful discussions regarding the results of their trenching studies within the Plunge Creek area. We thank Camille Bahri and Spring Pacific Properties for granting permission for the excavations we conducted for this study. Sinan Akciz, Jonathan Matti, Katherine Scharer, Lisa Grant Ludwig, and John Fletcher provided very helpful reviews of the manuscript. Amanda Lopez, Amanda Wilcox, and Joseph Salazar assisted with field work. James Budahn and Tim Debey conducted the NAA measurements. This is Southern California Earthquake Center Publication 1596.

REFERENCES CITED

Adamiec, G., and Aitken, M., 1998, Dose-rate conversion factors: Update: Ancient TL, v. 16, p. 37–50.

Anderson, M., Matti, J., and Jachens, R., 2004, Structural model of the San Bernardino basin, California, from analysis of gravity, aeromagnetic, seismicity data: Journal of Geophysical Research, v. 109, no. B4, B04404, doi:10.1029/2003JB002544, 20 p.

Becker, T.W., Hardebeck, J.L., and Anderson, G., 2005, Constraints on fault slip rates of the Southern California plate boundary from GPS velocity and stress inversions: Geophysical Journal International, v. 160, p. 634–650, doi:10.1111/j.1365-246X.2004.02528.x.

Behr, W.M., Rood, D.H., Fletcher, K.E., Guzman, N., Finkel, R., Hanks, T.C., Hudnut, K.W., Kendrick, K.J., Platt, J.P., Sharp, W.D., Weldon, R.J., and Yule, J.D., 2010, Uncertainties in slip-rate estimates for the Mission Creek strand of the southern San Andreas fault at Biskra Palms Oasis, Southern California: Geological Society of America Bulletin, v. 122, p. 1360–1377, doi:10.1130/B30020.1.

Bennett, R.A., Friedrich, A.M., and Furlong, K.P., 2004, Codependent histories of the San Andreas and San Jacinto fault zones from inversion of fault displacement rates: Geology, v. 32, no. 11, p. 961–964, doi:10.1130/G20806.1.

Bevis, M., Hudnut, K., Sanchez, R., Toth, C., Grejner-Brzezinska, D., Kendrick, E., Caccamise, D., Raleigh, D., Zhou, H., Shan, S., Shindle, W., Yong, A., Harvey, J., Borsa, A., Ayoub, F., Shrestha, R., Carter, B., Sartori, M., Phillips, D., and Coloma, F., 2005, The B4 Project: Scanning the San Andreas and San Jacinto Fault Zones: Eos (Transactions, American Geophysical Union, Fall Meeting Supplement), v. 86, p. F826, abstract H34B-01.

Birkeland, P.W., 1999, Soils and Geomorphology (3rd ed.): New York, New York, Oxford University Press, 430 p.

Blisniuk, K., Rockwell, T., Owen, L.A., Oskin, M., Lippincott, C., Caffee, M.W., and Dortch, J., 2010, Late Quaternary slip rate gradient defined using high-resolution topography and ^{10}Be dating of offset landforms on the southern San Jacinto fault zone, California: Journal of Geophysical Research, v. 115, B08401, doi:10.1029/2009JB006346.

Blisniuk, K., Oskin, M., Sharp, W., Rockwell, T., and Fletcher, K., 2011, Slip rates on the southern San Jacinto fault and Holocene–late Pleistocene kinematics of the Pacific–North American plate boundary: Southern California Earthquake Center Proceedings of the 2011 Annual Meeting, v. XXI, abstract A-152, p. 143.

Bronk Ramsey, C., 2009, Bayesian analysis of radiocarbon dates: Radiocarbon, v. 51, no. 1, p. 337–360.

DeMets, C., and Dixon, T.H., 1999, New kinematic models for Pacific–North America motion from 3 Ma to present: I. Evidence for steady motion and biases in the Nuvel-1A model: Geophysical Research Letters, v. 26, p. 1921–1924, doi:10.1029/1999GL900405.

Dolan, J.F., Bowman, D.D., and Sammis, C.G., 2007, Long-range and long-term fault interactions in Southern California: Geology, v. 35, p. 855–858, doi:10.1130/G23789A.1.

Fay, N.P., and Humphreys, E.D., 2005, Fault slip rates, effects of elastic heterogeneity on geodetic data, and the strength of the lower crust in the Salton Trough region, Southern California: Journal of Geophysical Research, v. 110, B09401, doi:10.1029/2004JB003548, 14 p.

Fialko, Y., 2006, Interseismic strain accumulation and the earthquake potential on the southern San Andreas

Downloaded from gsabulletin.gsapubs.org on January 7, 2013

fault system: Nature, v. 441, p. 968–971, doi:10.1038/nature04797.

Fletcher, K.E.K., Sharp, W.D., Kendrick, K.J., Behr, W.M., Hudnut, K.W., and Hanks, T.C., 2010, ^{230}Th/U dating of a late Pleistocene alluvial fan along the southern San Andreas fault: Geological Society of America Bulletin, v. 122, p. 1347–1359, doi:10.1130/B30018.1.

Harden, J.W., 1982, A quantitative index of soil development from field descriptions: Examples from a chronosequence in central California: Geoderma, v. 28, p. 1–28, doi:10.1016/0016-7061(82)90037-4.

Harden, J.W., and Matti, J.C., 1989, Holocene and late Pleistocene slip rates on the San Andreas fault in Yucaipa, California, using displaced alluvial-fan deposits and soil chronology: Geological Society of America Bulletin, v. 101, p. 1107–1117, doi:10.1130/0016-7606(1989)101<1107:HALPSR>2.3.CO;2.

Harden, J.W., and Taylor, E.M., 1983, A quantitative comparison of soil development in four climatic regimes: Quaternary Research, v. 20, p. 342–359, doi:10.1016/0033-5894(83)90017-0.

Horner, J.A., Rubin, C.M., and Lindvall, S.C., 2007, Slip rate studies along the Sierra Madre–Cucamonga fault system using ^{10}Be cosmogenic and geomorphic surface age analyses: Association of Environmental and Engineering Geologists Program with Abstracts (Geological Association of Canada), v. 50, p. 92.

Humphreys, E.D., and Weldon, R.J., II, 1994, Deformation across the western United States: A local estimate of Pacific–North America transform deformation: Journal of Geophysical Research, v. 99, p. 19,975–20,010, doi:10.1029/94JB00899.

Janecke, S.U., Dorsey, R.J., Forand, D., Steely, A.N., Kirby, S.M., Lutz, A.T., Housen, B.A., Belgarde, B., Langenheim, V.E., and Rittenour, T.M., 2010, High Geologic Slip Rates Since Early Pleistocene Initiation of the San Jacinto and San Felipe Fault Zones in the San Andreas Fault System, Southern California, USA: Geological Society of America Special Paper 475, 48 p.

Keller, E.A., Bonkowski, M.S., Korsch, R.J., and Shlemon, R.J., 1982, Tectonic geomorphology of the San Andreas fault zone in the southern Indio Hills, Coachella Valley, California: Geological Society of America Bulletin, v. 93, p. 46–56, doi:10.1130/0016-7606(1982)93<46:TGOTSA>2.0.CO;2.

Kendrick, K.J., Morton, D.M., Wells, S.G., and Simpson, R.W., 2002, Spatial and temporal deformation along the northern San Jacinto fault, Southern California; implications for slip rates: Bulletin of the Seismological Society of America, v. 92, p. 2782–2802, doi:10.1785/0120000615.

Kirby, S.M., Janecke, S.U., Dorsey, R.J., Housen, B.A., Langenheim, V.E., McDougall, K.A., and Steely, A.N., 2007, Pleistocene Brawley and Ocotillo Formations: Evidence for initial strike-slip deformation along the San Felipe and San Jacinto fault zones, Southern California: The Journal of Geology, v. 115, p. 43–62, doi:10.1086/509248.

Loveless, J.P., and Meade, B.J., 2011, Stress modulation on the San Andreas fault by interseismic fault system interactions: Geology, v. 39, p. 1035–1038, doi:10.1130/G32215.1.

Lundgren, P., Hetland, E.A., Liu, Z., and Fielding, E.J., 2009, Southern San Andreas–San Jacinto fault system slip rates estimated from earthquake cycle models constrained by GPS and interferometric synthetic aperture radar observations: Journal of Geophysical Research, v. 114, B02403, doi:10.1029/2008JB005996, 18 p.

Lutz, A.T., Dorsey, R.J., Housen, B.A., and Janecke, S.U., 2006, Stratigraphic record of Pleistocene faulting and basin evolution in the Borrego Badlands, San Jacinto fault zone, Southern California: Geological Society of America Bulletin, v. 118, p. 1377–1397, doi:10.1130/B25946.1.

Matmon, A., Schwartz, D.P., Finkel, R., Clemmens, S., and Hanks, T., 2005, Dating offset fans along the Mojave section of the San Andreas fault using cosmogenic ^{26}Al and ^{10}Be: Geological Society of America Bulletin, v. 117, p. 795–807, doi:10.1130/B25590.1.

Matti, J.C., and Morton, D.M., 1993, Paleogeographic evolution of the San Andreas fault in Southern California: A reconstruction based on a new cross-fault correlation, *in* Powell, R.E., Weldon, R.J., II, and Matti, J.C., eds., The San Andreas Fault System: Displacement, Palinspastic Reconstruction, and Geologic Evolution: Geological Society of America Memoir 178, p. 107–159.

Matti, J.C., Morton, D.M., and Cox, B.F., 1985, Distribution and Geologic Relations of Fault Systems in the Vicinity of the Central Transverse Ranges, Southern California: U.S. Geological Survey Open-File Report 85–365, 27 p., scale 1:250,000.

Matti, J.C., Morton, D.M., and Cox, B.F., 1992, The San Andreas Fault System in the Vicinity of the Central Transverse Ranges Province, Southern California: U.S. Geological Survey, Open-File Report 92–354, 40 p., scale 1:250,000.

Matti, J.C., Morton, D.M., Cox, B.F., Carson, S.E., and Yetter, T.J., 2003a, Geologic Map and Digital Database of the Yucaipa 7.5′ Quadrangle, San Bernardino and Riverside Counties, California, Version 1.0: U.S. Geological Survey Open-File Report 03–301, scale 1:24,000.

Matti, J.C., Morton, D.M., Cox, B.F., and Kendrick, K.J., 2003b, Geologic Map and Digital Database of the Redlands 7.5′ Quadrangle, San Bernardino and Riverside Counties, California, Version 1.0: U.S. Geological Survey Open-File Report 03–302, scale 1:24,000.

May, S.R., Repenning, C.A., and Cooper, J.D., 1982, New evidence for the age of the Old Woman Sandstone, Mojave Desert, California: Journal of Vertebrate Paleontology, v. 2, no. 1, p. 109–113, doi:10.1080/02724634.1982.10011921.

McCaffrey, R., 2005, Block kinematics of the Pacific–North America plate boundary in the Southwestern United States from inversion of GPS, seismological, and geologic data: Journal of Geophysical Research, v. 110, B07401, doi:10.1029/2004JB003307, 27 p.

McGill, S., Birnbaum, B.B., Burke, D., and Reeder, T., 1999, Late Quaternary activity on the north branch of the San Andreas fault, near San Bernardino, California, *in* Cranham, G.T., ed., Water for Southern California; Water Resources Development at the Close of the Century: San Diego, California, San Diego Association of Geologists, p. 31–36.

McGill, S., Dergham, S., Barton, K., Berney-Ficklin, T., Grant, D., Hartling, C., Hobart, K., McGill, J., Minnich, R., Rodriguez, M., Russell, J., Schmoker, K., Stumfall, M., Townsend, J., and Williams, J., 2002, Paleoseismology of the San Andreas fault at Plunge Creek, near San Bernardino, Southern California: Bulletin of the Seismological Society of America, v. 92, p. 2803–2840, doi:10.1785/0120000607.

McGill, S., Weldon R., and Owen, L., 2010, Latest Pleistocene slip rates along the San Bernardino strand of the San Andreas fault: Geological Society of America Abstracts with Programs, v. 42, no. 4, p. 69, paper 21-4.

Meade, B.J., and Hager, B.H., 2005, Block models of crustal motion in Southern California constrained by GPS measurements: Journal of Geophysical Research, v. 110, B03403, doi:10.1029/2004JB003209, 19 p.

Mejdahl, V., 1979, Thermoluminescence dating: Beta attenuation in quartz grains: Archaeometry, v. 21, p. 61–72, doi:10.1111/j.1475-4754.1979.tb00241.x.

Mezger, L.L., and Weldon, R.J., 1983, Tectonic implications of the Quaternary history of lower Lytle Creek, southeast San Gabriel Mountains: Geological Society of America Abstracts with Programs, v. 15, no. 5, p. 418.

Morton, D.M., 1975, Synopsis of the geology of the eastern San Gabriel Mountains, Southern California, *in* Crowell, J.C., ed., San Andreas Fault in Southern California: California Division of Mines and Geology Special Report 118, p. 170–176.

Morton, D.M., and Matti, J.C., 1987, The Cucamonga fault zone: Geologic setting and Quaternary history, *in* Recent Reverse Faulting in the Transverse Ranges, California: U.S. Geological Survey Professional Paper 1339, p. 179–203.

Morton, D.M., and Matti, J.C., 1993, Extension and contraction within an evolving divergent strike-slip fault complex; the San Andreas and San Jacinto fault zones at their convergence in Southern California, *in* Powell, R.E., Weldon, R.J., II, and Matti, J.C., eds., The San Andreas Fault System: Displacement, Palinspastic Reconstruction, and Geologic Evolution: Geological Society of America Memoir 178, p. 217–230.

Morton, D.M., and Matti, J.C., 2001, Geologic Map of the Devore 7.5-Minute Quadrangle, San Bernardino County, California: U.S. Geological Survey Open-File Report 01-173, version 1, scale 1:24,000.

Morton, D.M., Matti, J.C., Miller, F.K., and Repenning, C.A., 1986, Pleistocene conglomerate from the San Timoteo Badlands, Southern California; constraints on strike slip displacements on the San Andreas and San Jacinto faults: Geological Society of America Abstracts with Programs, v. 18, no. 2, p. 161.

Murray, A.S., and Wintle, A.G., 2000, Luminescence dating of quartz using an improved single-aliquot regenerative-dose protocol: Radiation Measurements, v. 32, p. 57–73, doi:10.1016/S1350-4487(99)00253-X.

Nicholson, C., Seeber, L., Williams, P., and Sykes, L.R., 1986, Seismicity and fault kinematics through the Eastern Transverse Ranges, California; block rotation, strike-slip faulting, and low-angle thrusts: Journal of Geophysical Research, v. 91, p. 4891–4908, doi:10.1029/JB091iB05p04891.

Noriega, G.R., Arrowsmith, J.R., Grant, L.B., and Young, J.J., 2006, Stream channel offset and late Holocene slip rate of the San Andreas fault at the Van Matre Ranch Site, Carrizo Plain, California: Bulletin of the Seismological Society of America, v. 96, p. 33–47, doi:10.1785/0120050094.

Orozco, A., 2004, Offset of a Mid-Holocene Alluvial Fan near Banning, CA; Constraints on the Slip Rate of the San Bernardino Strand of the San Andreas Fault [M.S. thesis]: Northridge, California, California State University at Northridge, 56 p.

Orozco, A., and Yule, D., 2003, Late Holocene slip rate for the San Bernardino strand of the San Andreas fault near Banning, California: Seismological Research Letters, v. 74, p. 237.

Oskin, M., Perg, L., Shelef, E., Strane, M., Gurney, E., Singer, B., and Zhang, X., 2008, Elevated shear zone loading rate during an earthquake cluster in eastern California: Geology, v. 36, p. 507–510, doi:10.1130/G24814A.1.

Powell, R.E., 1993, Balanced palinspastic reconstruction of pre–late Cenozoic paleogeology, Southern California; geologic and kinematic constraints on evolution of the San Andreas fault system, *in* Powell, R.E., Weldon, R.J., II, and Matti, J.C., eds., The San Andreas Fault System: Displacement, Palinspastic Reconstruction, and Geologic Evolution: Geological Society of America Memoir 178, p. 1–106.

Prentice, C.S., Weldon, R.J., and Sieh, K., 1986, Distribution of slip between the San Andreas and San Jacinto faults near San Bernardino, Southern California: Geological Society of America Abstracts with Programs, v. 18, no. 2, p. 172.

Prescott, J.R., and Hutton, J.T., 1994, Cosmic ray contributions to dose rates for luminescence and ESR dating: Large depths and long-term time variations: Radiation Measurements, v. 23, p. 497–500, doi:10.1016/1350-4487(94)90086-8.

Prescott, W.H., Savage, J.C., Svarc, J.L., and Manaker, D., 2001, Deformation across the Pacific–North America plate boundary near San Francisco Bay, California: Journal of Geophysical Research, v. 106, p. 6673–6682, doi:10.1029/2000JB900397.

Reimer, P.J., and 27 others, 2009, IntCal09 and Marine09 radiocarbon age calibration curves, 0–50,000 years cal BP: Radiocarbon, v. 51, no. 4, p. 1111–1150.

Rockwell, T., Loughman, C., and Merifield, P., 1990, Late Quaternary rate of slip along the San Jacinto fault zone near Anza, Southern California: Journal of Geophysical Research, v. 95, p. 8593–8605, doi:10.1029/JB095iB06p08593.

Sadler, P.M., and Trent, D.D., 1990, Geological transect of the central San Bernardino Mountains, Southern California, *in* Trent, D.D., coordinator, Guidebook, Geology of the Central San Bernardino Mountains, Southern California: Glendora, California, Spring Meeting Guidebook, Far Western Section, National Association of Geology Teachers, p. 36–68.

Salyards, S.L., Sieh, K.E., and Kirschvink, J.L., 1992, Paleomagnetic measurements of non-brittle deformation

Downloaded from gsabulletin.gsapubs.org on January 7, 2013

across the San Andreas fault at Pallett Creek: Journal of Geophysical Research, v. 97, p. 12,457–12,470, doi:10.1029/92JB00194.

Savage, J.C., and Prescott, W.H., 1978, Asthenosphere readjustment and the earthquake cycle: Journal of Geophysical Research, v. 83, p. 3369–3376, doi:10.1029/JB083iB07p03369.

Schoeneberger, P.J., Wysocki, D.A., Benham, E.C., and Broderson, W.D., 1998, Field book for describing and sampling soils: Lincoln, Nebraska, Natural Resources Conservation Service, USDA, National Soil Survey Center, 228 p.

Schwartz, D.P., and Weldon, R.J., 1986, Late Holocene slip rate on the Mojave segment of the San Andreas fault zone, Littlerock, CA; preliminary results: Eos (Transactions, American Geophysical Union), v. 67, p. 906.

Seeber, L., and Armbruster, J.G., 1995, The San Andreas fault system through the Transverse Ranges as illuminated by earthquakes: Journal of Geophysical Research, v. 100, p. 8285–8310, doi:10.1029/94JB02939.

Seitz, G., and Weldon, R., II, 1994, The paleoseismology of the southern San Andreas fault at Pitman Canyon, San Bernardino, California, *in* McGill, S.F., and Ross, T.R., eds., Geological Investigations of an Active Margin, Geological Society of America, Cordilleran Section Guidebook: Redlands, California, San Bernardino County Museum Association, p. 152–156.

Seitz, G., Weldon, R., II, and Biasi, G.P., 1997, The Pitman Canyon paleoseismic record: A re-evaluation of the southern San Andreas fault segmentation: Journal of Geodynamics, v. 24, p. 129–138, doi:10.1016/S0264-3707(96)00042-7.

Seong, Y.B., Owen, L.A., Bishop, M.P., Bush, A., Clendon, P., Copland, P., Finkel, R., Kamp, U., and Shroder, J.F., 2007, Quaternary glacial history of the central Karakoram: Quaternary Science Reviews, v. 26, p. 3384–3405, doi:10.1016/j.quascirev.2007.09.015.

Sharp, R.V., 1967, San Jacinto fault zone in the Peninsular Ranges of Southern California: Geological Society of America Bulletin, v. 78, p. 705–730, doi:10.1130/0016-7606(1967)78[705:SJFZIT]2.0.CO;2.

Sharp, R.V., 1981, Variable rates of late Quaternary strike-slip on the San Jacinto fault zone, Southern California: Journal of Geophysical Research, v. 86, p. 1754–1762, doi:10.1029/JB086iB03p01754.

Sieh, K., and Jahns, R.H., 1984, Holocene activity of the San Andreas fault at Wallace Creek, California: Geological Society of America Bulletin, v. 95, p. 883–896, doi:10.1130/0016-7606(1984)95<883:HAOTSA>2.0.CO;2.

Sieh, K., Grant, L.B., and Freeman, S.T., 1994, Late Quaternary slip rate of the north branch of the San Andreas fault at City Creek, California: Geological Society of America Abstracts with Programs, v. 26, no. 2, p. 91.

Soil Survey Staff, 2010, Keys to Soil Taxonomy (11th ed.): Washington, D.C., USDA-Natural Resources Conservation Service, 338 p.

Spinler, J.C., Bennett, R.A., Anderson, M.L., McGill, S.F., Hreinsdottir, S., and McCallister, A., 2010, Present-day strain accumulation and slip rates associated with southern San Andreas and Eastern California shear zone faults: Journal of Geophysical Research, v. 115, B11407, doi:10.1029/2010JB007424, 29 p.

Spotila, J.A., and Sieh, K., 2000, Architecture of transpressional thrust faulting in the San Bernardino Mountains, Southern California, from deformation of a deeply weathered surface: Tectonics, v. 19, p. 589–615, doi:10.1029/1999TC001150.

Stuiver, M., and Polach, H.A., 1977, Discussion; reporting of C-14 data: Radiocarbon, v. 19, p. 355–363.

Thatcher, W., 2009, How the continents deform: The evidence from tectonic geodesy: Annual Review of Earth and Planetary Sciences, v. 37, p. 237–262, doi:10.1146/annurev.earth.031208.100035.

U.S. Geological Survey and California Geological Survey, 2006, Quaternary Fault and Fold Database for the United States, USGS Web Site: http//earthquakes.usgs.gov/regional/qfaults/ (last accessed January 2010).

van der Woerd, J., Klinger, Y., Sieh, K., Tapponnier, P., Ryerson, F.J., and Meriaux, A., 2006, Long-term slip rate of the southern San Andreas fault from ^{10}Be-^{26}Al surface exposure dating of an offset alluvial fan: Journal of Geophysical Research, v. 111, B04407, doi:10.1029/2004JB003559, 17 p.

Weldon, R., 2010, Slip rate for the North Branch of the San Andreas fault, San Bernardino Valley, annual report to the Southern California Earthquake Center, http://sceccore2.usc.edu/proposalfiles/2010reports/Weldon_10108_report.pdf.

Weldon, R., and Humphreys, E.D., 1986, A kinematic model of Southern California: Tectonics, v. 5, p. 33–48, doi:10.1029/TC005i001p00033.

Weldon, R., Scharer, K., Fumal, T., and Biasi, G., 2004, Wrightwood and the earthquake cycle: What a long recurrence record tells us about how faults work: GSA Today, v. 14, no. 9, p. 4–10, doi:10.1130/1052-5173(2004)014<4:WATECW>2.0.CO;2

Weldon, R., Scharer, K.M., Sickler, R.R., Pruitt, A.H., Gilleland, C.L., and Garroway, J., 2008, Slip rate site on the San Andreas fault near Littlerock, California: Southern California Earthquake Center, 2008 Annual Meeting, Proceedings and Abstracts, v. 18, p. 167, abstract 2–053.

Weldon, R.J., II, 1986, Late Cenozoic Geology of Cajon Pass: Implications for Tectonics and Sedimentation along the San Andreas Fault [Ph.D. dissertation]: Pasadena, California, California Institute of Technology, 400 p.

Weldon, R.J., II, and Sieh, K.E., 1985, Holocene rate of slip and tentative recurrence interval for large earthquakes on the San Andreas fault, Cajon Pass, Southern California: Geological Society of America Bulletin, v. 96, p. 793–812, doi:10.1130/0016-7606(1985)96<793:HROSAT>2.0.CO;2.

Weldon, R.J., II, Meisling, K.E., and Alexander, J., 1993, A speculative history of the San Andreas fault in the central Transverse Ranges, California, *in* Powell, R.E., Weldon, R.J., II, and Matti, J.C., eds., The San Andreas Fault System: Displacement, Palinspastic Reconstruction, and Geologic Evolution: Geological Society of America Memoir 178, p. 161–198.

Wesnousky, S.G., Prentice, C.S., and Sieh, K., 1991, An offset Holocene stream channel and the rate of slip along the northern reach of the San Jacinto fault zone, San Bernardino Valley, California: Geological Society of America Bulletin, v. 103, p. 700–709, doi:10.1130/0016-7606(1991)103<0700:AOHSCA>2.3.CO;2.

Yule, D., 2009, The enigmatic San Gorgonio Pass: Geology, v. 37, p. 191–192, doi:10.1130/focus022009.1.

Yule, D., and Sieh, K., 2003, Complexities of the San Andreas fault near San Gorgonio Pass: Implications for large earthquakes: Journal of Geophysical Research, v. 108, no. B11, 2548, doi:10.1029/2001JB000451, 23 p.

Yule, D., and Spotila, J., 2010, Quaternary geology of the San Bernardino Mountains and their tectonic margins, *in* Clifton, E.H., and Ingersoll, R.V., eds., Geologic Excursions in California and Nevada: Tectonics, Stratigraphy and Hydrogeology: Upland, California, Pacific Section SEPM (Society for Sedimentary Geology), Book 108, p. 273–322.

Yule, D., Fumal, T., McGill, S., and Seitz, G., 2001, Active tectonics and paleoseismic record of the San Andreas fault, Wrightwood to Indio: Working toward a forecast for the next "Big Event," *in* Dunne, G., and Cooper, J., compilers, Geologic Excursions in the California Deserts and Adjacent Transverse Ranges, Fieldtrip Guidebook and Volume prepared for the Joint Meeting of the Cordilleran Section Geological Society of America and the Pacific Section American Association of Petroleum Geologists, 9–11 April 2001: Universal City, California, Pacific Section SEPM (Society for Sedimentary Geology), p. 91–126.

Science Editor: Nancy Riggs
Associate Editor: John M. Fletcher

Manuscript Received 23 November 2011
Revised Manuscript Received 22 March 2012
Manuscript Accepted 12 April 2012

Printed in the USA